JAISCR, 2024, Vol. 14, No. 4, pp. 321 – 359
10.2478/jaiscr-2024-0018

QUANTUM CHIMP OPTIMIZATION ALGORITHM: A NOVEL INTEGRATION OF QUANTUM MECHANICS INTO THE CHIMP OPTIMIZATION FRAMEWORK FOR ENHANCED PERFORMANCE

Meng Yu[1], Mohammad Khishe[2*,3,4], Leren Qian[5], Diego Martín[6],
Laith Abualigah[7,8,9,10], Taher M. Ghazal[11]

[1]*School of Artificial Intelligence, Anshan Normal University, Anshan, 114005, China*

[2]*Department of Electronic Engineering, Imam Khomeini Naval Science University of Nowshahr, Iran*

[3]*Applied Science Research Center, Applied Science Private University, Amman 11937, Jordan*

[4]*Innovation Center for Artificial Intelligence Applications, Yuan Ze University, Taiwan*

[5]*School of Computing and Augmented Intelligence, Arizona State University, Tempe 85281, AZ, USA*

[6]*ETSI Telecomunicación, Universidad Politécnica de Madrid, Av. Complutense 30, 28040 Madrid, Spain*

[7]*Computer Science Department, Al al-Bayt University, Mafraq 25113, Jordan*

[8]*MEU Research Unit, Middle East University, Amman 11831, Jordan*

[9]*Jadara Research Center, Jadara University, Irbid 21110, Jordan*

[10]*Centre for Research Impact & Outcome, Chitkara University, Punjab, India*

[11]*Center for Cyber Security, Faculty of Information Science and Technology, Universiti Kebangsaan Malaysia (UKM), 43600 Bangi, Selangor, Malaysia*

**E-mail: m_khishe@alumni.iust.ac.ir*

Submitted: 7th February 2024; Accepted: 1st July 2024

Abstract

This research introduces the Quantum Chimp Optimization Algorithm (QChOA), a pioneering methodology that integrates quantum mechanics principles into the Chimp Optimization Algorithm (ChOA). By incorporating non-linearity and uncertainty, the QChOA significantly improves the ChOA's exploration and exploitation capabilities. A distinctive feature of the QChOA is its ability to displace a 'chimp,' representing a potential solution, leading to heightened fitness levels compared to the current top search agent. Our comprehensive evaluation includes twenty- nine standard optimization test functions, thirty CEC-BC functions, the CEC06 test suite, ten real-world engineering challenges, and the

IEEE CEC 2022 competition's dynamic optimization problems. Comparative analyses involve four ChOA variants, three leading quantum-behaved algorithms, three state-of-the-art algorithms, and eighteen benchmarks. Employing three non-parametric statistical tests (Wilcoxon rank-sum, Holm-Bonferroni, and Friedman average rank tests), results show that the QChOA outperforms counterparts in 51 out of 70 scenarios, exhibiting performance on par with SHADE and CMA-ES, and statistical equivalence to jDE100 and DISHchain1e+12. The study underscores the QChOA's reliability and adaptability, positioning it as a valuable technique for diverse and intricate optimization challenges in the field.

Keywords: statistical analysis, engineering application, Chimp optimization algorithm, quantum optimization

1 Introduction

In the swiftly advancing domain of computational optimization [1–3], the convergence of quantum computing principles and nature-inspired algorithms offers a promising frontier characterized by abundant possibilities [4]. Quantum computing is renowned for its exceptional computational power and ability to execute several tasks simultaneously, offering a groundbreaking approach to solving complex optimization problems [5, 6]. The revolutionary framework utilizes the distinctive characteristics of quantum physics, including superposition and entanglement, to investigate solution spaces with unparalleled efficacy [7, 8]. The incorporation of quantum principles into nature-inspired algorithms is becoming increasingly attractive as the demand for more advanced optimization approaches rises [9], particularly in scenarios that involve extensive and complex datasets. The combination of these algorithms not only improves the capabilities of classic methods but also creates opportunities for the development of innovative approaches that may effectively address the intricacies of contemporary optimization problems [10–12].

Benioff and Feynman proposed the concept of quantum computing in the early 1980s, arguing that quantum-based computers outperformed their classical equivalents when solving particular problems [13]. Feynman suggested using quantum mechanics to solve computational issues [14]. Based on this reference, issues that classic computers cannot solve can be solved by primary quantum machines simulating sophisticated quantum systems. The idea of a quantum Turing machine was then introduced, and reference [15] provided a theoretical demonstration of the possibility of universal representations based on quantum physics. Reference [16] provides the first quantum algorithm. Subsequently, Cerezo et al. [17] introduced quantum algorithms that demonstrate the superiority of quantum computing over conventional computers in tackling specific tasks. These particular issues, meanwhile, were handcrafted, and as a result, they have only a marginally practical impact.

In 1994, Shor proposed factoring big integers [18]. The cryptographical security of the Rivest-Shamir-Adleman (RSA) is ensured by sizeable prime factorization, an NP-hard issue. Utilizing conventional computers, it takes exponentially more time to tackle this issue [19]. However, the Shor technique demonstrates that just polynomial time is required with quantum computing, making RSA easily crackable. The Grover quantum searching technique can thus successfully locate a specific piece of information in an unsorted database [20]. Grover's approach can verify all data simultaneously at each turn by utilizing quantum parallelism, significantly decreasing the difficulty of solving this search problem. The novel computing approach and enormous possibilities for information processing offered by quantum computing have drawn much attention since the Shor and Grover algorithms were proposed.

The design of algorithms has been significantly impacted by quantum computation [21]. There is much worry about integrating quantum computing's robust storage and analysis advantages into current optimization algorithms. Since nature-inspired algorithms have long been widespread [22, 23], including chaotic Henry gas solubility optimization algorithm [24], chaotic Lévy flight distribution optimization algorithm [25], african vultures optimization algorithm for optimization [26], artificial gorilla troops algorithm [27], and hunger games search algorithm [28], it makes sense to suggest merging quantum theory with these techniques [29, 30]. By leveraging the principles of quantum parallel processing, the limitations inherent in nature-inspired programs can be efficiently mitigated [31].

This work focuses on the task of enhancing the rate at which optimization algorithms converge while simultaneously avoiding their entrapment in local minima. We suggest employing ChOA, a nature-inspired optimization method renowned for its simplicity and efficacy in diverse optimization situations. Nevertheless, ChOA may have difficulties while dealing with intricate situations and get trapped in local optima. In order to address this constraint, we propose the incorporation of a quantum mechanism (QM) to augment the performance of ChOA. The QChOA technique seeks to achieve a harmonious equilibrium between exploration and exploitation, which is a crucial undertaking in metaheuristic algorithms. By attaining this balance, we allow the algorithm to effectively navigate the range of possible solutions, discover innovative solutions, and enhance its ability to optimize hard issues by improving upon promising areas.

The sections of this paper are as follows: Section 2 presents a comprehensive review of related works. The basics of ChOA are discussed in Section 3. In Section 4, we provide a comprehensive description of the QChOA. Section 5 discusses QChOA and its application to testing benchmark functions and engineering problems. The final section provides a brief conclusion and some directions for the future.

2 Literature review

There are several existing quantum intelligent algorithms, such as the quantum co-evolution algorithm (QCA) [32, 33], the quantum- behaved simulated annealing (QSA) [34], the quantum whale optimization algorithm (QWOA) [35], the quantum recurrent encoder- decoder neural network (QREDNN) [36], the Quantum-inspired ant lion optimizer (QALO) [37], the probabilistic quantum clustering (PQC) [38], the quantum probability-inspired graph attention network (QGAN) [39], the quantum differential evolution (QDE) [40], the quantum grey wolf optimizer (QGWO) [41], the quantum particle swarm optimization algorithm (QPSO) [42, 43], the quantum- behaved sparse dictionary learning (QSDL) [44], the quantum annealing algorithm (QAA) [45]. Table 1 presents the comparative characteristics of quantum-inspired optimization techniques.

These algorithms incorporate the advantages of quantum computing by being designed to align with the characteristics of quantum mechanisms or drawing inspiration from them. Because of the significant delay in the advancement of quantum hardware, it is not possible to evaluate these algorithms on an actual quantum computer. Nevertheless, through the process of modeling quantum computing, these algorithms can showcase their superiority over traditional algorithms inspired by nature.

Motivated by previous studies [32, 34, 35, 37, 40–43, 45], we recommend incorporating the quantum computing concept into the classical ChOA [47] to improve its performance.

In 2020, Khishe introduced a nature-inspired ChOA technique [47]. The algorithm relies on certain swarm behaviors exhibited by groups of chimpanzees during the hunting operation to find optimal or near-optimal solutions. Researchers and industrial experts have used the ChOA in three major research categories since its introduction in 2020:

In the first category, the ChOA has tried to address a wide range of real-world optimization problems and mathematical equations, such as:

- *COVID-19 Diagnosis* [48]: ChOA has demonstrated promise in providing precise illness diagnosis. However, the availability of large and high-quality data for training and validation may be a determining factor in its effectiveness.

- *Time Series Prediction* [49]: When used with time series data, ChOA can produce precise forecasts. On the other hand, treating data sensitivity and model generalization carefully may be necessary.

- *Multi-level Thresholding Segmentation* [50]: Although ChOA has enhanced picture segmentation, the implementation of the algorithm may become more complex.

Table 1. Comparative characteristics of quantum-inspired optimization techniques

Algorithm	**Disadvantages**	**Advantages**	**Research Gap Addressed in Quantum-behaved Version**
QCA [33]	Slow convergence	Efficient for binary problems	Enhanced convergence using quantum interference
QPSO [43]	Limited exploration capability	Improved exploration and exploitation	Improved exploration and exploitation of quantum concepts
QSA [34]	Temperature schedule choice	Improved exploration and exploitation	Enhanced quantum-inspired exploration and exploitation
QACO [46]	High computational cost	Rapid convergence for small problems	Integration of quantum principles in ant colony optimization
QALO [37]	Slow for large-scale problems	High precision	Quantum speed-up for large-scale optimization
PQC [38]	Requires large quantum depth	Quantum-assisted clustering	Improved scalability with quantum techniques
QWOA [35]	Complexity due to hybrids	update mechanisms	Improved search and update mechanisms
QGAN [39]	Requires complex training data	Quantum-based feature extraction	Quantum-enhanced training method
QDE [40]	Prone to getting stuck in local minima	Quick adaptation to the environment	Enhanced quantum-based global search
QSDL [44]	Requires high quantum depth	efficiency in dictionary learning	Improved quantum depth handling
QGWO [41]	Hardware limitations	Quantum-inspired exploration	Integration of quantum concepts for optimization

- *Haptic Brief Appearance Framework* [51]: Although ChOA improves haptic feedback systems, system and hardware constraints may prevent it from being implemented fully.

- *Simultaneous Feature Selection* [52]: For feature selection, ChOA can be applied to improve model performance. However, high-dimensional data might run into issues with scalability and processing complexity.

- *Fuzzy Cluster Analysis* [53]: Cluster analysis is improved by ChOA via fuzzification. It might, however, be susceptible to the selection of fuzzification parameters.

- *Data Clustering* [54]: Cluster analysis is enhanced by ChOA; however, because of its complexity, precise parameter tuning may be necessary.

- *Environmental Power Dispatch Problem* [55]: Although ChOA maximizes power dispatch, system dynamics, and environmental conditions may have an impact on it.

- *Multi-Sensor Computation* [56]: Although ChOA enhances multi-sensor data fusion, its adaptation to various sensor types might need to be taken into account.

- *Oil-Gas Recovery* [57]: Although ChOA improves hydrocarbon recovery, oil and gas operations in the real world are complicated and uncertain.

- *Intelligent Robots* [58]: ChOA improves robotic systems' intelligence; however, in practical implementations, hardware and implementation issues could arise.

- *Sonar Dataset Target Detection and Recognition* [59]: Target detection and recognition are enhanced by ChOA; however, robustness to handle noisy data may be needed.

- *Minimizing Power Loss of Distribution Networks* [60]: Although ChOA lowers power loss in distribution networks, it may not be easy to handle complexity and network scale issues.

- *Design of Tunnel FET Architectures* [61]: Although there is potential for energy-efficient designs utilizing ChOA, there may be restrictions due to design specifications.

- *Color image enhancement* [62]: This method uses bilateral gamma correction to improve the contrast of the image further while using ChOA to choose the incomplete Beta function's parameter values adaptively.

While these research projects hold value, pursuing innovative paradigms or employing novel techniques as initial approaches to address a well-established problem may not constitute robust research directions. Table 2 provides a summary of the applications of ChOA in practical scenarios, along with their respective merits and drawbacks.

In the second category, the ChOA is merged with other methods to increase efficiency and productivity, such as:

– *Hybrid Whale optimization algorithm and ChOA (WOA-ChOA)* [63]: It aims to boost efficiency and productivity in duties pertaining to optimization. The solution space can be efficiently explored by the new search techniques made possible by the connection with WOA. However, the extra complexity of the hybrid method needs to be considered in real use.

– *Hybrid ChOA-Hunger Game Search* [64]: The hunger game search (HGS) algorithm and ChOA are combined in this hybrid method. It seeks to improve exploitation and exploration capabilities through integration with HGS. Nevertheless, the hybrid algorithm's additional complexity needs to be carefully controlled, particularly in situations with limited computational resources.

– *Hybrid ChOA-Cuckoo Search* [65]: This hybrid method combines the cuckoo search (CS) method with ChOA. It aims to enhance the exploitation and exploration of the solution space through the integration of CS. When using this hybrid strategy, it is imperative to take into account the trade-off between optimization advantages and algorithm complexity.

– *Spotted Chimp Hybrid Optimization Algorithm* (SChOA) [66]: SChOA is an additional hybridization that combines search strategies inspired by spotted hyenas with ChOA. Through the combination of two tactics, this hybridization seeks to improve overall performance. However, it is essential to consider how hybridization has increased complexity.

– *Crossbred Random Forests ChOA (CRF- ChOA)* [67]: In this version, ChOA is combined with random forests (RF), an accuracy-focused machine learning approach. The goal of the RF integration is to increase task accuracy in optimization. The complexity that is added by combining these two approaches is the trade-off.

Other hybrid models are random vector functional link network (RVFL)-ChOA [68], hybrid dragonfly ChOA [69], and the SChOA [70]. Although the proposed hybrid algorithms significantly increased accuracy, their fundamental drawback is their enormous complexity. The summary of hybrid models and their advantages and disadvantages is presented in Table 3.

These hybrid algorithms indeed offer advantages in terms of accuracy, efficiency, and productivity. However, their increased complexity should be considered in practical applications, especially when computational resources are limited. Careful parameter tuning and performance evaluation are essential to harness the benefits of these hybrid approaches effectively.

In summary, the second category of ChOA variants involves hybrid algorithms that combine ChOA with other optimization techniques to improve performance. While they offer advantages, such as enhanced accuracy and efficiency, their complexity needs to be managed and evaluated in the context of specific optimization tasks.

Finally, in the third category, In an effort to enhance the performance of the ChOA, researchers undertook the task of inventing and tweaking a range of operators. As an illustration:

– *Fuzzy*ChOA [71]: FuzzyChOA introduces fuzzification to fine-tune ChOA's variables. This modification enhances adaptability and fine-tuning capabilities, making ChOA better suited for complex optimization tasks. However, it may add some computational complexity to the algorithm.

– *Opposition-Based Lévy Flight* ChOA *(IChOA)* [50]: In order to improve the transition between the exploitation and exploration phases, this version includes opposition-based Lévy flight behavior. It is more capable of exploring and exploiting the solution space, which increases its

Table 2. The summary of the applications of ChOA in real-world problems.

Application	Disadvantages	Advantages
COVID-19 Diagnosis [48]	May require extensive data and validation	Potential for accurate disease diagnosis
Multi-level Thresholding Segmentation [50]	Algorithm complexity	Improved image segmentation
Time Series Prediction [49]	Data sensitivity and model generalization	Potential for accurate predictions
Simultaneous Feature Selection [52]	Complexity and scalability issues	Feature selection for improved model performance
Haptic Brief Appearance Framework [51]	Hardware and implementation constraints	Enhanced haptic feedback system
Data Clustering [54]	Algorithm complexity	Improved cluster analysis
Fuzzy Cluster Analysis [53]	Algorithm sensitivity to fuzzification	Enhanced cluster analysis
Multi-sensor computation [56]	Algorithm adaptability to sensor types	Improved multi-sensor data fusion
Environmental Power Dispatch Problem [55]	Sensitivity to environmental factors	Optimized power dispatch
Oil-Gas Recovery [57]	Real-world complexities	Improved hydrocarbon recovery
Minimizing Power Loss of Distribution Networks [60]	Complexity and network size	Reduced power loss in networks
Sonar Dataset Target Detection and Recognition [59]	Data quality and noise issues	Enhanced target detection and recognition
Design of Tunnel FET Architectures [61]	Algorithm-specific design constraints	Potential for energy-efficient designs
Intelligent Robots [58]	Hardware and implementation challenges	Enhanced intelligence in robotic systems
Color image enhancement [62]	Need bilateral gamma correction	Adaptively select the parameter values

Table 3. Comparative characteristics of ChOA and its hybrid variants

Algorithm	Disadvantages	Advantages	Improvements
dragonfly ChOA [69]	Increased complexity	Enhanced exploration and exploitation	Integration with Dragonfly for better balance
CRF-ChOA [67]	Enormous complexity	Improved accuracy through hybrids	Integration with random forests for accuracy
SChOA [66]	Complexity due to hybridization	Improved accuracy with hybridization	Integration with spotted hyena-inspired search
WOA-ChOA [63]	Increased complexity	Enhanced efficiency and productivity	Integration with whale optimization for productivity
ChOA-HGS [64]	Increased complexity	Enhanced exploration and exploitation	Integration with Hunger game search for diversity
ChOA-CS [65]	Increased complexity	Improved exploration and exploitation	Integration with cuckoo search for optimization
RVFL-ChOA [68]	Complexity due to hybridization	Enhanced performance through hybridization	Integration with RVFL

robustness. For best outcomes, users might need to adjust some parameters.

– *Quadratic Mutation* ChOA *(QSA)* [72]: In order to launch a species with a quadratic mutation, QSA uses Spearman's rank value of the lowest-ranking chimps in society. Optimization performance is enhanced by this method, primarily when used in conjunction with ChOA. Nevertheless, it could result in a more sophisticated algorithm.

– *Weighted* ChOA *(W*ChOA*)* [73]: To accelerate convergence, WChOA suggests averaging chimpanzees in a weighted manner. Although it streamlines the optimization process, precise parameter tuning might be necessary to get the best outcomes.

– *Dynamic Levy Flight* ChOA *(DLF*ChOA*)* [74]: To facilitate the best possible transition between the exploration and exploitation phases of ChOA, DLFChOA implements dynamic Levy flight. Although this adjustment increases the adaptability of the algorithm, it may also increase computing complexity.

– *Combined with Cuckoo Search and Selective Opposition (SOCS*ChOA*)* [75]: Cuckoo search, selective opposition, and ChOA are combined in SOCSChOA to enhance overall optimization performance. It offers a more thorough and efficient investigation of the solution space. However, cautious management of the additional complexity resulting from hybridization is necessary.

– *Refraction Learning* ChOA *(RL-ChOA)* [76]: Refraction learning, an opposition- based learning mechanism based on the physical principle of light refraction, is introduced by RL-ChOA. It accelerates convergence and raises population variability. However, because of its unique process, it might result in additional computing costs.

– *Enhanced* ChOA *(EChOA)* [77]: This version uses an adjustable weight somersault foraging strategy to improve ChOA for 3D route planning. Somersault foraging and the adaptive weight— obtained from the coefficient vector of ChOA —help avoid local optima and enhance early-stage population diversity. Still, it adds another level of intricacy.

– *Multi-strategy ChOA (MSChimp)* [78]: To achieve this equilibrium between exploration and exploitation, ChOA implemented an opposition-based learning approach during its initialization phase to increase population diversity and a Sine Cosine Algorithm (SCA) during its later exploitation phase to boost the algorithm's convergence speed and accuracy.

The summary of improved models and their advantages and disadvantages is presented in Table 4.

In the third category of ChOA variants, researchers have focused on enhancing ChOA's performance by introducing various modifications and operators to the algorithm. While these modifications and operators have demonstrated relative advantages in enhancing specific aspects of ChOA's performance, they also come with potential drawbacks, such as increased complexity or the need for parameter tuning. Therefore, researchers and practitioners should carefully assess the suitability of these variants for their specific optimization tasks, considering the trade-offs involved.

Although the methods mentioned above had relative advantages in one of the phases of extraction or exploitation or adjusting the relationship between these two phases, practically, they helped increase the speed of convergence or avoid local optima. Although some algorithms, such as DLFChOA and SOCSChOA, showed promising results in both phases, they had high time complexity.

Motivations: The shortcomings mentioned above, on the one hand, and the no free lunch theory [79], on the other hand, motivated us to look for a combined technique to simultaneously improve both the exploration and exploitation phases so that the convergence rate increases and the optimizer do not get stuck in local minima.

The reason for choosing ChOA among other newly presented nature-inspired and swarm-based optimization algorithms is its simple math, the low number of setting parameters, and the ability of this algorithm in many optimization problems. However, it frequently becomes stuck at a local optimum when attempting to handle intricate issues. Our work presents the quantum mechanism (QM),

Table 4. The advantages and disadvantages of ChOA and its improved version (3^{rd} category)

Algorithm	Disadvantages	Advantages	Enhancement
FuzzyChOA [71]	May introduce additional complexity	Enhanced adaptability and fine-tuning	Fuzzification
IChOA [50]	May require parameter tuning	Enhanced exploration and exploitation	Opposition-based Lévy flight
QSA [72]	Potential increase in algorithm complexity	Improved optimization performance	Quadratic mutation and Spearman's rank
WChOA [73]	May require careful parameter tuning	Increased convergence speed	Weighted averaging of chimpanzees
DLFChOA [74]	May introduce computational complexity	Improved transition between exploration and exploitation	Dynamic Levy flight
SOCSChOA [75]	Increased complexity due to hybridization	Improved overall optimization performance	Combined with cuckoo search and selective opposition
RL-ChOA [76]	Potential for increased computational cost	Increased population variability and convergence speed	Refraction learning
EChOA [77]	Complexity due to adaptive weight and somersault foraging	Enhanced exploration and exploitation	Somersault foraging with adaptive weight
MSChimp [78]	Potential for increased computational cost	Enhanced exploration and exploitation	opposition-based learning and SCA

a novel approach to enhance ChOA's performance on complex optimization tasks.

Achieving a balance between exploration and exploitation is a crucial and challenging task in metaheuristic algorithms, including the QChOA that has been presented. It is essential to achieve this balance to ensure that the algorithm can effectively explore the solution space to discover new and potentially better solutions, while also taking advantage of already promising areas to further enhance the solutions. In the context of QChOA, the following approach is employed to tackle this challenge:

Incorporating Quantum Concepts: QChOA utilizes quantum computing techniques to augment its exploration and exploitation skills. Quantum computing inherently exhibits parallelism, allowing for the simultaneous investigation of several solutions. Using parallelism during the exploration phase facilitates the algorithm's ability to broaden its search by concurrently searching multiple places inside the solution space.

Non-Linearity and Uncertainty: The use of non-linearity and uncertainty, which are fundamental characteristics of quantum physics within the QChOA framework, inject elements of randomness and variety into the search process. Utilizing non-linearity within the approach allows it to navigate the solution space in a non-linear manner, hence aiding in the avoidance of local optima. The inclusion of uncertainty in decision-making introduces a degree of randomization, preventing the algorithm from being confined to suboptimal regions.

Population Diversity: Preserving diversity within a population is of utmost importance to obtain a harmonious equilibrium between exploitation and exploration. QChOA implements strategies to maintain a diversified population of candidate solutions. The presence of diversity inside the algorithm facilitates the exploration of a broad spectrum of potential solutions, hence mitigating the risk of early convergence.

Dynamic Adaptation: The search strategy employed by QChOA is subject to continuous adaptation in response to the optimization process. This adaptation involves the dynamic adjustment of parameters to manage the exploration and exploitation trade-off effectively. To illustrate, the algorithm may enhance exploration by introducing higher randomness if it detects rapid convergence or intensifies exploitation when it identifies the discovery of promising regions.

Constraint Handling: In the context of real engineering applications, it is frequently necessary to adhere to certain constraints to achieve desired outcomes. The QChOA framework incorporates a novel constraint- handling technique for effectively managing constraints. This constraint-handling technique ensures that the method does not excessively prioritize exploration to the detriment of fulfilling the problem's restrictions.

Benchmarking and Analysis: In order to optimize the trade-off between exploration and exploitation, the QChOA algorithm undergoes thorough benchmarking and analysis using a wide range of test functions and real-world engineering problems. This thorough evaluation enhances our understanding of the algorithm's effectiveness in various contexts and allows us to make suitable adjustments to its parameters.

In summary, QChOA combines quantum concepts, introduces randomness through non- linear and uncertain elements, maintains a diverse population, adapts its strategy dynamically, and includes constraint management to address the exploration-exploitation problem. By combining these methodologies, QChOA is able to efficiently balance the exploration and exploitation trade- off, making it a viable tool for solving complex optimization issues in real-world situations.

Because of this, the following are the paper's most significant contributions:

Contribution:

- We present QChOA, a quantum-based variant of the classical ChOA that improves upon the classical algorithm's flexibility and speed of convergence.
- The QChOA incorporates the non- linearity and uncertainty concepts into the current ChOA to place a chimp far away from the population, resulting in an agent with superior fitness than the present best agent.
- To address the drawbacks of constrained engineering optimization problems that arise in real-world settings, QChOA provides a novel constraint-handling technique.

29 conventional benchmark functions, 30 complicated CECBC functions, ten functions of the CEC06 test suit, and ten real-world application-based engineering challenges are used to conduct in-depth analyses of the merits of the proposed QChOA. The QChOA is evaluated against four groups of standard optimization approaches, including (1) DLFChOA [74], ULChOA [80], NChOA [81], and IChOA [77] as novel variants of ChOA, (2) QGWO [41], QWOA [35], and QSA [34] as the three best quantum behaved techniques, (3) SHADE [82], CMAES [82], and LSHADE-SPACMA [83] as the three well-known optimization algorithms, and jDE100, DISHchain1e+12, CIPDE, and EBOwithCMAR as best performing algorithms in IEEE CEC competition [83]. A comprehensive evaluation is carried out using three non-parametric statistical tests: Wilcoxon rank sum [84], Holm's sequential Bonferroni procedure [85], and Friedman-type rank tests [86] The findings reveal that the QChOA ranked top among 46 out of 70 test functions and engineering challenges and displayed comparable outcomes to SHADE and CMAES in other comparisons. The analytical research showed that QChOA is statisticall comparable to jDE100 and DISHchain1e+12 while being a much better optimizer than the benchmark algorithms for the three first categories.

3 Related Terminology: Chimp Optimization Algorithm

In a chimpanzee group, there are four distinct roles that individuals might take on: attacker, barrier, chaser, and driver. They each bring unique skills to a meal that are essential for hunting. Finally, the attacker estimates the prey's escape path, leading it to return to the driver or go down into the lower canopy, while the barriers position one another in the canopy in order to prevent the escape of prey. The chaser follows the prey rather than endeavoring to capture it. Successful hunters are rewarded with a massive piece of meat since it is believed that attackers require more intelligence to forecast the actions of their target. An attacker plays a crucial role, and it increases with maturity, intelligence, and strength. In exchange for social rewards, including group support and courting, chimpanzees have been proven to engage in meat hunting. After the hunt, all the chimpanzees abandon their assigned tasks in favor of acquiring meat as quickly as possible, a chaotic outcome driven by their underlying social motivation (sexual desire). Chimps typically split their hunting activity into two stages: the exploration stage, which entails behaviors like barriering, chasing, and driving prey, and the exploitation stage, which entails attacking prey. The ChOA is based on swarm intelligence and is designed to mimic the collaborative predation habits of chimpanzee groups in the wild [47].

3.1 Exploration Phase (Chasing and Ariving Prey)

The initial phase in catching prey is the technique of chasing prey, Equations (1) to (4) can describe [47]:

$$\mathbf{p}_{chimp}^{t+1} = \mathbf{p}_{prey}^{t} - \kappa \cdot |\mathbf{J} \cdot \mathbf{p}_{prey}^{t} - \zeta \cdot \mathbf{p}_{chimp}^{t}| \quad (1)$$

$$\kappa = 2 \cdot \beta \cdot r_1 - \beta \quad (2)$$

$$J = 2 \cdot (r_2) \quad (3)$$

$$\zeta = according to chaotic maps \quad (4)$$

Where p_{prey} is the best solution found thus far, p_{chimp} indicates the best chimpanzee position, t represents the number of iterations, κ, J, and ζ represents the coefficient vectors. Furthermore, where r_1 and r_2 represent random numbers between 0 and 1, it is worth noting that these coefficients and translations are described in detail in reference [47].

3.2 Exploitation Phase (Attacking Prey)

Due to our ignorance about the precise location of our initial meal, the greatest and first chimpanzee strategy is to use prey in order to mimic our behavior statistically. After ChOA stores the top four chimps, the other chimps will be compelled to relocate in relation to where the top four chimps are located, as decided by Eqs. (5) and (6) [47].

$$p_{t+1} = \frac{1}{4} \times (p_1 + p_2 + p_3 + p_4) \quad (5)$$

Where

$$\begin{aligned} p_1 &= p_A - a_1 \cdot |c_1 p_A - \mathbf{m}_1 \mathbf{x}| \\ p_2 &= p_B - a_2 \cdot |c_2 p_B - \mathbf{m}_2 \mathbf{x}| \\ p_3 &= p_C - a_3 \cdot |c_3 p_C - \mathbf{m}_3 \mathbf{p}| \\ p_4 &= p_D - a_4 \cdot |c_4 p_D - \mathbf{m}_4 \mathbf{p}| \end{aligned} \quad (6)$$

3.3 Sexual Motivation (Social Incentive)

At the conclusion of the hunting expedition, the four subspecies of chimpanzees interact, and the chimps' social motivations (group support, courting) temporarily relieve them of their hunting duties. So they attempted to coerce their way into the supply of chaotic flesh. Further alleviating issues like local optimization and sluggish convergence when addressing high dimensional problems is achieved by the algorithm's chaotic pattern during the last stage. Table 5 shows all six of the chaotic maps that were utilized in the paper. These maps show systems that are both stochastic and deterministic. To account for both phenomena, we assume that, during optimization, chimpanzees' locations can be updated by either the standard positionupdating mechanism or the chaotic model with equal probability. Equation (7) gives the mathematical form of its model.

$$\mathbf{p}^{t+1} = \begin{cases} \text{Eq. (5)} & \eta_m < 0.5 \\ \zeta & \eta_m \geq 0.5 \end{cases} \quad (7)$$

Where $\eta_m$is an arbitrary integer between zero and one. This oversimplified perspective on learning, however, may cause modest or early convergence. To fix these issues, we propose a quantum mechanism in the section that follows. Using the same strategy, we can expand the search region to D dimensions and have the chimpanzees move in a hyperbolic shape (or hyperspheres) around the best spot we have found so far.

4 Proposed Methodology: A Quantum-behaved Chimp Optimization Algorithm

When an agent uses a quantum-based search method (instead of a Newtonian random walk), the resulting search space analysis can reveal the most advantageous locations. It is feasible due to the possibility that some search agents will occur at a great distance from a given site. Searching agents in the quantum-based search space should move in the D-dimensional Hilbert space instead of the Newtonian space and have a potential quantum field to assure the constraint state for preventing the explosion and, by extension, ensure convergence.

Table 5. The Chaotic maps used in ChOA

No	Name	Chaotic map	Range
1	Tent	$x_{i+1} = \begin{cases} \frac{10 \times x_i}{7} & x_i < 0.66 \\ \frac{10}{3}(1-x_i) & 0.66 \leq x_i \end{cases}$	(0,1)
2	Logistic	$x_{i+1} = 4 \times (1 - x_i \times x_i$	(0,1)
3	Gauss/mouse	$x_{i+1} = \begin{cases} 1 & x_i = 0 \\ \frac{1}{mod(x_i,1)} & otherwise \end{cases}$	(0,1)
4	Singer	$x_{i+1} = 1.08 \times (7.86x_i - 23.31x_i^2 + 28.75x_i^3 - 13.30x_i^4)$	(0,1)
5	Quadratic	$x_{i+1} = x_i^2 - 1$	(0,1)
6	Bernoulli	$x_{i+1} = 2 \times x_i(mod1)$	(0,1)

Conventional ChOA's mathematical model shows that the algorithm's convergence is dependent on the positions of each chimp, which change in response to the roles of the barrier, attacker, chaser, and driving chimps with the final update by Equation (5), where p^{t+1} denotes the average position of the top four chimps. It follows that a chimp's local draw is determined by the average of the top four chimps as well as by the positions of each individual. For $\upsilon = 1, 2, ..., \psi$ chimps' population, the local movement of each chimpanzee can be expressed as $W_\upsilon^t = (w_{\upsilon,1}^t, w_{\upsilon,2}^t, \ldots, w_{\upsilon,DIM}^t)$, where t denotes the iteration, and DIM denotes the number of variables (dimension) associated with the problem. Thus, Equation (8) can express the local attractor positions for the w^{th} chimp and d^{th} dimension at the t iteration.

$$\begin{aligned} w_{\upsilon,d}^t =& \kappa_A \times p_{Ave,d}^t \\ &+ (1-J_A)p_{A,d}^t + (1-J_B)p_{B,d}^t \\ &+ (1-J_C)p_{C,d}^t + (1-J_D)p_{D,d}^t \\ p_{Ave,d}^t =& \frac{1}{4} \times (p_A + p_B + p_C + p_D) \end{aligned} \tag{8}$$

Where $p_{Ave,d}^t$ denotes the average position of the top four chimpanzees for the d^{th} dimension (attacker, barrier, chaser, and driver). As defined in the original ChOA, the parameter κ and J can be similarly stated. The value of the κ_A, which can be changed to balance the algorithm's global and local search capability, is employed to drive the attack more towards the direction of the attacker chimp. Adding the term $(1 - J_k)$ to Equation (8) will cause the associated chimp to move in the negativ and positive directions as follows randomly:

$$(1-J_k) = \begin{cases} -di, & if rand < \frac{1}{2} \\ 0, & if rand = \frac{1}{2} \\ +di, & if rand > \frac{1}{2} \end{cases} \tag{9}$$

The chimps' present attacker, barrier, chaser, driver positions, and average positions all approach a single point, which causes the ChOA to converge globally. The essential time-dependent Schrödinger equation for quantum mechanics is given by Equations (10) and (11):

$$\lambda \frac{\partial \Theta(P,t)}{\partial t} = -\widehat{\Gamma}(P)\Theta(P,t) \tag{10}$$

$$\widehat{\Gamma}(P) = -\frac{\lambda^2}{2\upsilon}\nabla^2 + \Pi(P) \tag{11}$$

Where υ stands for the chimpanzee's mass λ, denotes the Planck constant, and $\Pi(P)$ represents the potential energy distribution. In Equation (10), the wave function $\Theta(P,t)$ describes the chimpanzee's quantum state and solely depends on the chimpanzee's position. It has no direct physical significance. Its amplitude squared $\Theta(.)^2$ in a four-dimensional space establishes a probability measure by solving the following equation:

$$\Theta(P,t)^2 dxdydz = \varpi dxdydz \tag{12}$$

Where $\varpi dxdydz$ represents the likelihood that a chimpanzee will appear in the threedimensional space around the location (x, y, z). In other words,

$\Theta(P,t)^2$ is the probability density function (PDF) fitting Equation (13).

$$\int\int\int_Y \Theta(P,t)^2\, dxdydz = \int\int\int_Y \varpi dxdydz = 1 \tag{13}$$

The statistical analysis of the wave function is represented by Equations (12) and (13), where the integral is carried across the entire space. Every chimpanzee in the method has been given a spinless motion in D-dimensional Hilbert space with a specific potential field (energy). The chimp is pulled using this field by a location specified in Equation (8). This potential field produces bound states according to quantum physics and ought to be centered at zero. For moving the chimpanzees in the constrained domain of the search space, the most basic delta potential that is well-oriented at g is considered. The potential field is given by Equation (14) for onedimensional Hilbert space (D = 1), where the chimpanzee's location is considered as P and w^t_υ as w .

$$\begin{cases} \Upsilon = -\zeta\cdot\delta(P-w) = -\zeta\cdot\delta(\Omega) \\ \Omega = P-w \end{cases} \tag{14}$$

Where ζ is the prospective well's depth. At the center, it is infinite, and everywhere else, it is zero. For D-dimensional Hilbert space, the technique to implement QChOA can be calculated, in which each dimension of the chimpanzees' location is constrained by a delta potential well and adjusted individually. In order to measure the $d^th(1 \le d \le DIM)$ dimension of the mth $(1 \le \vartheta \le \psi)$ chimp position for the $(t+1)^{th}$ iteration, we can use the update equation obtained for QPSO in reference [42] as follows:

$$P^{t+1}_{\upsilon,j} = w^t_{\upsilon,d} \pm \frac{\chi^t_{\upsilon,d}}{2} Ln(\frac{1}{T^{t+1}_{\upsilon,d}}) \tag{15}$$

Where $T^{t+1}_{\upsilon,d}$ denotes a series of random integers distributed uniformly across the interval (0,1) and change with time for each υ and d. Equation (16) represents the value of $\chi^t_{\upsilon,d}$

$$\chi^t_{\upsilon,d} = 2\cdot l\cdot P^t_{\upsilon,d} - g^t_d \tag{16}$$

$g^t = g^t_1, g^t_2, \dots, g^t_{DIM}$

Where g^t denote the chimpanzee's average positions at iteration t, as determined by Equation (17):

$$g^d_t = \frac{1}{\Psi}\sum_{\upsilon=1}^{\Psi} P^t_{\upsilon,d} \tag{17}$$

Lastly, the QChOA position update equation can be derived as follows:

$$P^{t+1}_{\upsilon,d} = w^t_{\upsilon,d} \pm l\cdot P^t_{\upsilon,d} - g^t_d\,(\frac{1}{T^{t+1}_{\upsilon,d}}) \tag{18}$$

$$l = \frac{1}{2} - (\frac{t}{max(t)}) \tag{19}$$

In its most fundamental form, the QChOA is shown by Equation (18). This context makes sense when we talk about the positions that the words "attacker," "barrier," "chaser," and "driver" describe. The parameter "l" in the current study is linearly adjusted during iterations between $-\frac{1}{2}$ and $\frac{1}{2}$. According to Equation (19), it has a positive value during the initial half of the iterations and a negative value during the following half. Figure 1 depicts the proposed QChOA block diagram.

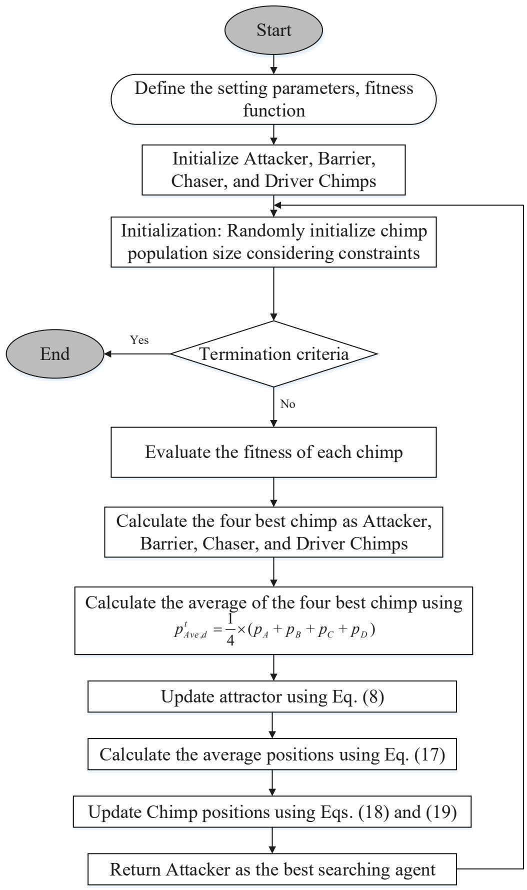

Figure 1. QChOA's block diagram

5 Experimentation and Analysis

This section presents a comparative analysis of the performance of the suggested QChOA in relation to established methodologies. In this context, the utilization of three distinct categories of evaluation functions is employed in conjunction with a single collection of ten practical engineering optimization tasks:

1. Fixed-dimension multi-modal, multi-modal, and unimodal are the three standard test function categories.
2. There are thirty complex compositional and hybrid functions in the most recent and most difficult numerical optimization competition CECBC2017 test sets.
3. The 100Digit Challenge CEC062019 [87], which has ten functions. Take note that the best answer offered for the ten processes is the value 1.000000000.
4. 10 real-world Engineering Problems from CEC2020 [88].
5. Benchmark for dynamic optimization problems produced by generalized moving peaks at the 2022 IEEE CEC.

Various test functions are used in this research to test the effectiveness of the QChOA. The typical baseline functions utilized to evaluate the potential of QChOA for exploitation, exploration, and avoiding getting stuck in local minima are the unimodal (UM) [89], multimodal (MM), Fixed-dimension multi-modal (FDM) [90], and composition functions (CFs) [91]. The primary objective of UM functions is to assess the algorithm's susceptibility to exploitation. The MM functions are used as a means of measuring exploration performance. Fifty dimensions are used to evaluate the two groups mentioned above of functions. The efficacy of QChOA in overcoming local optima is evaluated by conducting experiments with a range of CFs, specifically F24 to F29. The FDM benchmark functions, which vary between F14 and F23, demonstrate the ability of QChOA to explore in low dimensions. CFs are used to test the algorithm's effectiveness because their complexity is the same as realworld tasks since they contain many local optima. Figure 2 displays the twodimensional representation of several test functions.

A maximum of 25,000 function evaluations and 500 iterations are used to tackle the benchmark functions using QChOA and other different approaches. The research study involved doing 30 rounds of the QChOA in order to obtain statistically significant findings. The outcomes of each iteration were recorded and analyzed as a function of the standard deviation (Std) and average (Ave) values of the most optimal responses obtained thus far.

Twelve popular metaheuristic methods were tested in the study, including DLFChOA [74], ULChOA [80], QSA [34], NChOA [81], IChOA [77], QGWO [41], QWOA [35], jDE100 [92], DISHchain1e+12, CIPDE[1] [93], EBOwithCMAR[2] [94], and standard ChOA to prove the merit of QChOA over other benchmark methods. Each evaluation is performed on a PC equipped with Win 11, 16 GB of RAM, a Core i7 processor that clocks in at 3.8 GHz, and Matlab R2020a. The various parameters of the comparison algorithms are described in Table 6. The utilized setup parameters fall in the permitted range for achieving the highest possible efficiency across all algorithms or precisely advised by their respective inventors.

5.1 The Performance Analysis of Exploitation Feature

They can evaluate the exploitation of QChOA's potential since only one global optimum in UM exists. The results of QChOA and various optimization techniques on UMs (F1-F7) utilizing Ave and Std metrics are shown in Table 7. A non-parametric statistical procedure called Wilcoxon's rank-sum testing was utilized to find out if the QChOA results differed significantly from other assessments [84]. It should be noted that 5% was chosen as the significance level in this instance. In addition to AVE and STD, the research outcomes also present the p-values obtained from Wilcoxon's test. The abbreviation "N/A" signifies "Not Applicable," indicating that the technique is unsuitable as this test cannot contrast the most suitable algorithm with itself. The

[1] Collective Information Powered Differential Evolution
[2] Effective Butterfly Optimizer with Covariance Matrix Adapted Retreat phase

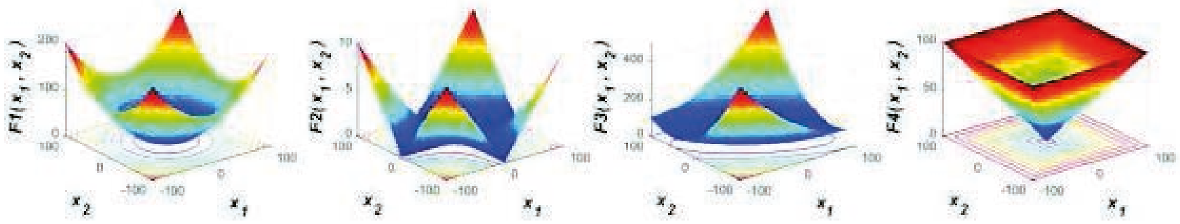

a) UM benchmark function

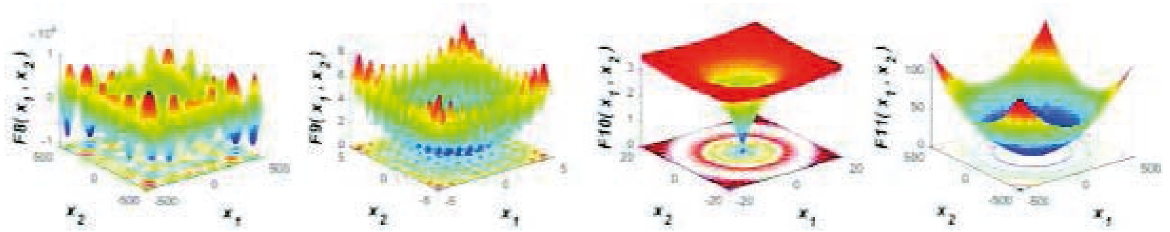

b) MM benchmark function

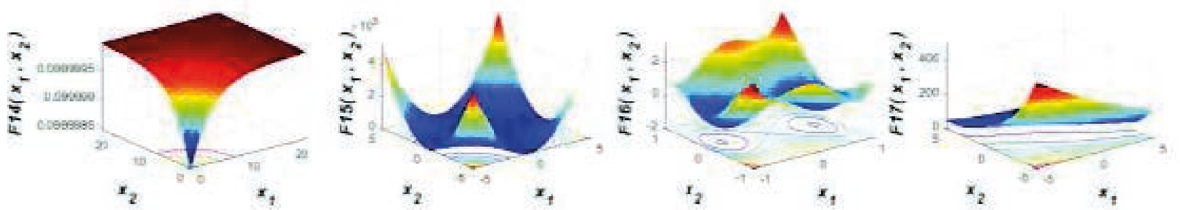

c) FDM benchmark function

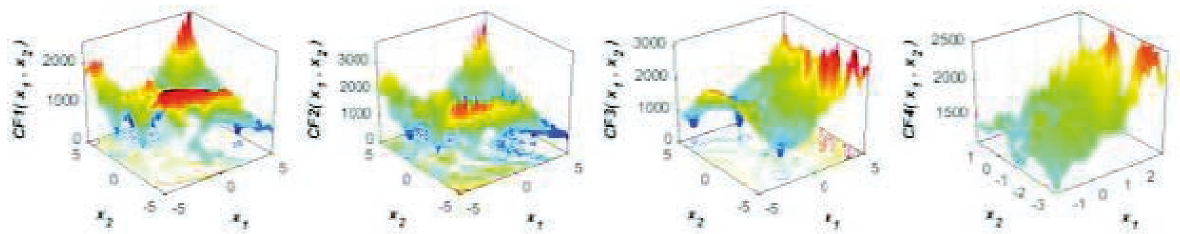

d) CFs

Figure 2. Twodimensional representation of several test functions.

Table 6. Setting parameters for the utilized algorithm

Algorithm	Parameter	Value
ChOA & its variants	f	[2,0)
	m	Chaos
QGWO	a	linearly varied between 0.5 and 0.5
QWOA	selection	Roulette wheel
	crossover	Single point
	mutation rate	0.01
jDE100 & DISHchain1e+12	CR	0.8
	F	0.4
CIPDE	F	0.6
	CR	0.4
	c	0.12
	T	250
	RT	1950
EBOwithCMAR	CR, freq	0.4
	F	0.6
	T	0.1

Table 7. The results of UM functions.

Algorithm		F_1	F_2	F_3	F_4	F_5	F_6	F_7
ChOA	Ave	7.89E-08	7.44E19	1.90E-07	1.55E-03	48.441	3.50E-04	3.89E-03
	Std	7.55E-08	6.53E23	1.89E-07	1.96E-03	39.331	3.50E-04	3.89E-03
	p-value	0.00033	0.0055	0.0051	0.0073	0.0068	0.0025	0.0030
ULChOA	Ave	1.44E12	0.00331	1.02E-07	1.33E-04	51.455	8.32E03	1.53E-03
	Std	7.53E-09	0.00023	1.44E-07	1.75E-04	33.785	5.33E03	1.11E-03
	p-value	0.0055	0.0044	0.0025	0.0039	0.0056	0.0051	0.0082
IChOA	Ave	6.96E12	2.11E07	1.42E08	1.22E09	48.335	1.32E02	3.22E03
	Std	6.44E-08	3.33E08	0.0017E07	1.11E06	33.045	5.14E03	2.02E03
	p-value	0.0033	0.0035	0.0014	0.0013	0.0055	0.0072	0.0083
NChOA	Ave	2.01E27	2.11E08	3.2E08	1.21E08	47.236	1.33E12	1.07E03
	Std	1.21E55	8.42E07	1.25E06	1.11E07	35.443	2.55E06	2.51E03
	p-value	0.0015	0.0044	0.0025	0.0039	0.0073	0.0051	0.0082
DLFChOA	Ave	3.11E40	7.11E23	5.11E09	3.53E08	63.220	7.25E06	1.49E03
	Std	6.06E40	6.35E23	1.90E08	1.12E09	33.116	4.25E07	6.06E02
	p-value	0.0033	0.0044	0.0055	0.0056	0.0071	0.0025	0.0030
QSA	Ave	6.44E07	5.41E21	0.98E06	1.15E08	76.350	1.42E07	1.89E03
	Std	4.11E07	6.44E23	1.90E08	1.12E09	33.045	5.14E03	2.02E03
	p-value	0.0055	0.0047	0.0025	0.0039	0.0056	0.0051	0.0082
QCChOA	Ave	1.14E33	1.78E23	3.88E11	1.42E09	2.41	1.45E04	1.05E03
	Std	0.0000	1.54E35	2.34E11	1.12E09	2.41	1.14E07	1.05E04
	p-value	N/A	N/A	N/A	N/A	N/A	N/A	N/A
QGWO	Ave	4.35E14	4.33E14	1.90E08	1.12E09	76.350	1.42E07	1.89E03
	Std	1.33E16	1.35E16	1.90E08	1.12E09	33.045	5.14E03	2.02E03
	p-value	0.0055	0.0047	0.0025	0.0039	0.0056	0.0051	0.0082
QWOA	Ave	1.07E07	0.0036	3.88E07	1.32E06	75.350	1.11E03	7.29E-03
	Std	7.00E-07	0.0076	3.88E07	1.32E06	33.045	1.14E07	1.11E03
	p-value	0.0044	0.0055	0.0025	0.0039	0.0056	0.0051	0.0082
SHADE	Ave	1.23E19	3.22E19	2.20E04	1.33E11	1.31E01	1.42E07	1.05E04
	Std	2.11E37	1.15E12	1.10E05	1.12E09	3.14E01	1.45E07	1.05E04
	p-value	0.0055	0.0055	0.0025	0.0039	0.0056	0.0051	0.0082
CMAES	Ave	2.05E31	0.00E+00	1.25E09	1.09E09	2.07E16	1.11E07	2.02E03
	Std	1.23E33	0.00E+00	1.10E05	1.12E09	3.14E01	1.45E07	1.05E04
	p-value	N/A	N/A	N/A	N/A	N/A	N/A	N/A
LSHADE-SPACMA	Ave	0.7537	2.52E12	2.52E09	1.14E08	51.291	1.42E07	7.20E03
	Std	1.23E19	1.52E19	1.10E05	1.12E09	3.14E01	1.45E07	1.05E04
	p-value	0.0055	0.0055	0.0025	0.0039	0.0056	0.0051	0.0082

bold style of the p-values indicates little difference between the two algorithms.

Numbers in bold represent the best performance achieved for each metric in each experiment. Based on the findings, it can be observed that QChOA exhibited superior performance compared to the majority of competing algorithms across all test functions, with the exception of F6 and F7, in which it attained a second-place ranking. The findings of this study illustrate the potential for exploitation of the quantum mathematical notion, which allows the QChOA to efficiently and accurately converge towards the global optimum.

5.2 The Performance Analysis of Exploration Feature

The evaluation of an algorithm's capacity for exploration is conducted using MM functions, as they can exhibit numerous local optima based on the layout parameters. All of the test functions in F8F23 are multi-modal and come in both MM and FDM types. The outcomes of the QChOA and other techniques for such tasks are presented in Tables 8 and 9. Numbers in bold represent the best performance achieved for each metric in each experiment.

These tables show that, among the methods, the QChOA has the best capacity for exploration. QChOA demonstrates superior performance contrasted to other techniques for 50% of the MMs, while for the others, as modern optimizers, it produces competitive results. The level of accuracy achieved by QChOA in FDMs is analogous to that of state- of-the-art optimization techniques in attaining the optimal solution in most cases. The different stages of optimization that go into QChOA's exploration capability impact this improvement due to the QM capability.

5.3 The Local Optima Avoidance Capability

F24-F29 is the CF that is obtained by using rotating, shifting, and combination operations on basic UM and MM functions. CFs are produced to evaluate the methods' ability to avoid local minima and strike a good balance between exploration and exploitation. It can be seen how well the QChOA and other optimization techniques perform in CFs in Table 10. The outcomes indicate that QChOA is more effective than competing methods. The outcomes reveal that the QChOA algorithm is well-balanced between the exploration and exploitation phases and that it is able to avoid local optima quite well by means of the thorough relocation process that QM facilitates. Table 11 employs Friedman's mean rank test to ascertain the cumulative rank of the benchmark algorithms. As indicated in Table 11, QChOA demonstrated the highest ranking in comparison to the other benchmark techniques. Numbers in bold represent the best performance achieved for each metric in each experiment.

5.4 QChOA's Convergence Analysis

This section delves into the experimental convergence of the QChOA. To evaluate the convergence of QChOA, we employ measures including average fitness history, converging graphs, and trajectories. For the performance and convergence investigation of QChOA in several benchmark test functions, these metrics are displayed in Figure 3. The 2D illustration of benchmarks regarding this figure is indicated in the 1^{st} column, which might help comprehend the function's domain architecture.

One of the earliest metrics to reveal the top outcome up to this point is the convergence curve. Convergence curves in UM functions follow a smooth pattern, consistent across all categories, which indicates improving outcomes with time. This trend, however, transforms into the regular stepwise pattern for MM and CFs. It is clear from each category that, for UM functions, QChOA can initially encompass the ideal point and then iteratively improve the results. On the contrary, even in the final rounds, participants in MM and CFs achieved better outcomes by doing a global search throughout the search region. This strategy results in curves resembling steps, with little progress even after a few MM functions have been applied. It is observed that the exploratory performance depends on the agents' QM factor in the most recent iterations. Once the searching agents are viewed as colony members, the best individual's behavior in maximizing the colony's success may be noticed in the convergence graph. However, no data is available about the entire colony's performance. This shortcoming is the rationale behind choosing the average fitness history statistic as an additional in-

Table 8. The results of MM functions.

Algorithm		***F8***	***F9***	***F10***	***F11***	***F12***	***F13***
ChOA	Ave	−1.07E+04	3.39E−07	**7.33E-16**	**0.00E 00**	4.30E-06	3.09E-01
	Std	1.22E+03	3.39E−07	**7.25E-16**	**0.00E 00**	4.30E-06	3.09E-01
	p-value	0.0033	0.0055	**N/A**	0.0022	0.0035	0.0045
ULChOA	Ave	−1.25E+04	1.25E−07	**7.33E16**	**0.00E 00**	1.01E-04	2.10E-04
	Std	0.1	3.22E−07	3.22E−07	**0.00E 00**	1.30E-04	8.50E-04
	p-value	0.0077	0.0082	0.0035	0.0041	0.0033	0.0071
IChOA	Ave	−1.12E+04	1.4423	2.0441	0.0002	2.01E-03	2.22E-04
	Std	1766.46	0.3000	0.1001	0.0033	2.02E-03	1.33E-04
	p-value	0.0011	0.0047	0.0032	0.0015	0.00001	0.0017
NChOA	Ave	−1.03E+04	1.11E−04	0.8223	1.01E-05	1.30E-05	2.10E-05
	Std	555.233	3.45E−04	0.0021	1.00E-05	1.25E-05	1.50E-05
	p-value	0.0072	0.0082	0.0035	0.0041	0.0033	0.0071
DLFChOA	Ave	−9.03E+03	2.22E−07	8.21E14	**0.00E 00**	7.88E07	2.92E-03
	Std	595.1113	2.11E−07	2.44E14	**0.00E 00**	7.88E07	1.44E-03
	p-value	0.0033	0.0042	0.0035	0.0047	0.0047	0.0015
QSA	Ave	−1.33E+04	0.0933	2.12E15	1.01E-07	7.12E04	3.94E-07
	Std	796.12698	0.0322	2.33E14	1.30E-07	0.0031	1.22E-03
	p-value	0.0035	0.0042	0.0086	0.0032	0.0036	0.0091
QChOA	Ave	**−1.75E+04**	**0.00E 00**	1.88E13	**0.00E 00**	**0.00E 00**	**0.00E 00**
	Std	**525.5351**	**0.00E 00**	1.44E12	**0.00E 00**	**0.00E 00**	**0.00E 00**
	p-value	**N/A**	**N/A**	0.0017	**N/A**	**N/A**	**N/A**
QGWO	Ave	−1.38E+04	1.1335	9.33E12	**0.00E 00**	8.30E-04	2.11E-03
	Std	742.6746	0.3440	6.17E12	**0.00E 00**	7.44E-04	1.02E-03
	p-value	0.0076	0.0042	0.0086	0.0032	0.0036	0.0091
QWOA	Ave	−1.42E+04	0.3007	0.9003	**0.00E 00**	2.10E-04	5.10E-04
	Std	715.5351	0.1001	0.1335	**0.00E 00**	8.50E-04	2.30E-04
	p-value	0.0063	0.0082	0.0035	0.0041	0.0033	0.0071
SHADE	Ave	−8.83E+03	0.029	0.1702	1.01E-04	1.19E-04	1.01E-04
	Std	418.8	0.831	0.0244	1.22E-04	3.90E-04	1.00E-04
	p-value	0.0077	0.0025	0.0035	0.0032	0.0033	0.0071
CMAES	Ave	−1.16E+04	0.0085	6.044	**0.00E 00**	**1.13E14**	1.25E12
	Std	331.3	0.0344	2.706	**0.00E 00**	**1.25E13**	1.11E12
	p-value	0.0035	0.0042	0.0055	0.0032	0.0044	0.0091
LSHADE-SPACMA	Ave	−1.32E+04	0.0023	0.1525	9.01E-05	0.0008	2.11E-06
	Std	454.325	0.0016	0.0188	9.30E-05	0.0019	1.04E-08
	p-value	0.0065	0.0082	0.0040	0.0041	0.0033	0.0071

Table 9. The results of FDM functions.

Algorithm		***F14***	***F15***	***F16***	***F17***	***F18***	***F19***	***F20***	***F21***	***F22***	***F23***
	Ave	2.3332	3.05E−04	1.0359	0.4005	3.000022	3.8544	3.21003	10.133	10.333	10.45
ChOA	Std	0.0911	3.02E−04	6.32E−14	1.33E06	1.21E09	1.47E10	2.44E02	2.04E02	2.77E02	2.11E02
	p-value	0.0033	0.0025	0.0014	0.0032	0.0045	0.0073	0.0044	0.0042	0.0075	0.0088
	Ave	1.0444	3.54E−04	1.0449	0.3989	3.000019	3.8633	3.29622	10.122	10.421	10.531
IChOA	Std	0.2731	6.32E−04	2.11E−12	7.11E11	2.44E12	1.42E13	1.66E10	2.13E02	3.33E04	2.55E02
	p-value	0.0044	0.0047	0.0021	0.0011	0.0025	0.0066	0.0025	0.0077	0.0065	0.0063
	Ave	1.0305	2.20E−04	1.0355	0.4033	3.00000	3.8621	3.2901	6.155	10.322	10.522
IChOA	Std	1.0001	3.32E−04	5.11E−09	0.4033	3.00000	3.8655	3.2608	2.77E02	3.13E01	2.75E02
	p-value	0.0028	0.0073	0.0014	0.0032	0.0032	0.0073	0.0071	0.0042	0.0066	5.11E−09
	Ave	0.9645	3.29E−04	1.0384	0.3995	3.000042	3.8622	3.28876	10.133	9.4033	10.510
NChOA	Std	1.22E14	4.02E−04	4.73E15	5.12E14	1.88E14	2.77E15	1.22E10	2.66E08	2.11E02	5.11E−09
	p-value	0.0044	0.0047	0.0021	0.0011	0.0025	0.0066	0.0025	0.0077	0.0065	0.0063
	Ave	0.1033	3.21E−04	1.0362	0.3925	3.00012	3.7954	3.19001	7.544	9.320	9.6501
DLFChOA	Std	1.22E14	6.52E−04	6.15E15	9.36E14	1.88E13	4.11E15	1.60E08	1.44E02	1.23E01	7.11E−02
	p-value	0.0011	0.0033	0.0021	0.0011	0.0021	0.0066	0.0088	0.0077	0.0015	0.0063
	Ave	1.1330	2.11E06	1.0352	0.3989	3.000045	3.8636	3.28654	**10.165**	10.421	10.520
QSA	Std	2.8713	3.33E04	2.38E−09	9.36E13	2.40E02	1.25E14	1.85E10	2.33E05	2.77E02	8.15E−03
	p-value	0.0033	0.0025	0.0014	0.0032	0.0045	0.0073	0.0044	0.0042	0.0075	0.0088
	Ave	**1.08E−05**	**3.01E−04**	**1.03161**	0.3972	**3.000001**	**3.8645**	3.0004	**10.165**	9.4077	**10.537**
QChOA	Std	**1.09E−17**	**3.08E15**	**4.03E18**	9.02E15	**1.33E16**	**2.41E15**	**1.11E11**	**2.1E11**	2.25E11	**3.62E11**
	p-value	**N/A**	**N/A**	**N/A**	**0.0577**	**N/A**	**N/A**	**0.00184**	**N/A**	0.0033	**N/A**
	Ave	0.9333	3.02E−04	1.0341	0.3996	3.000033	3.8633	3.2899	10.122	**10.4041**	10.536
QGWO	Std	2.33E15	4.09E−04	4.46E16	9.12E15	1.46E14	1.46E14	1.14E11	2.53E11	2.38E−09	3.91E11
	p-value	0.0033	0.0025	0.0014	0.0032	0.0045	0.0073	0.0044	0.0042	0.0075	0.0088
	Ave	1.0002	3.64E−04	1.0357	0.3991	3.000033	3.8644	1.992	6.144	7.477	6.5322
QWOA	Std	1.0044	6.66E−04	6.85E−14	8.22E13	1.32E13	3.11E13	1.13E09	2.25E02	2.38E−09	0.0033
	p-value	0.0066	0.0047	0.0055	0.0011	0.0025	0.0066	0.0023	0.0057	0.0065	4.11E−06
	Ave	0.8827	1.25E03	**1.0316**	0.3983	3.000025	3.8628	3.0334	9.1344	**10.414**	**10.537**
SHADE	Std	**3.41E16**	5.22E03	0.0033	1.12E16	3.14E15	1.46E14	5.77E02	1.1325	2.63E11	9.00E11
	p-value	**0.054**	0.0022	**0.054**	0.0033	0.0025	0.0014	0.0032	0.0045	0.0073	**0.052**
	Ave	1.0335	3.02E−04	**1.0316**	**0.3982**	3.9900	3.8628	**3.2903**	7.1410	**10.414**	**10.537**
CMAES	Std	0.2044	1.19E−04	**6.22E17**	**0.0000**	1.33E+01	2.51E15	1.44E11	3.4120	**2.02E11**	5.11E−09
	p-value	0.0033	0.0033	**0.066**	**N/A**	0.0035	0.00001	**N/A**	0.0003	**N/A**	**0.066**
	Ave	0.9044	1.44E03	**1.0316**	0.3988	3.000041	3.8628	3.0333	9.1436	**10.435**	**10.537**
LSHADE-SPACMA	Std	3.21E16	5.32E03	0.0033	1.11E16	3.22E14	1.33E14	5.77E02	1.2269	2.44E11	9.11E11
	p-value	**0.054**	0.0033	0.0025	0.0014	0.0032	0.0045	0.0073	0.0044	0.0042	0.0075

Table 10. The results of CFs.

Algorithm		**F24 (CF1)**	**F25 (CF2)**	**F26 (CF3)**	**F27 (CF4)**	**F28 (CF5)**	**F29 (CF6)**
	Ave	63.2201	198.221	283.1423	392.2145	198.2214	807.3355
ChOA	Std	75.2001	58.2214	87.0745	88.251	98.5213	100.073
	p-value	0.0033	0.0023	0.0043	0.0021	0.0013	0.0017
	Ave	37.5421	135.3225	212.321	266.3021	183.556	699.4123
ULChOA	Std	50.1332	89.5213	32.5514	89.03212	99.3256	109.85215
	p-value	0.0019	0.0033	0.0011	0.0039	0.0022	0.0025
	Ave	67.553	89.5213	311.365	60.3356	85.1444	720.08236
IChOA	Std	95.802	57.4122	38.2574	95.1444	105.0884	197.3521
	p-value	0.0047	0.0024	0.0032	0.0017	0.00022	0.0037
	Ave	44.2255	72.3355	295.6625	133.2541	92.1358	690.07621
NChOA	Std	43.399	39.152	77.521	122.1358	92.1358	63.9631
	p-value	0.0019	0.0035	0.0011	0.0022	0.0017	0.0025
	Ave	67.5213	88.2214	145.225	302.3521	49.5588	701.2014
DLFChOA	Std	84.3322	44.1332	41.2811	66.2569	33.7745	189.3026
	p-value	0.0033	0.0025	0.0043	0.0021	0.0035	0.0017
	Ave	32.4421	65.3214	198.3214	311.1111	132.447	729.204
QSA	Std	19.2136	23.6145	45.3321	101.5569	88.7541	88.2369
	p-value	0.0019	0.0043	0.0022	0.0021	0.0017	0.0025
	Ave	6.1133	14.0021	137.852	273.133	2.1124	88.2145
QCChOA	Std	11.2211	22.0000	16.021	24.1003	1.2341	39.5541
	p-value	N/A	N/A	N/A	N/A	N/A	N/A
	Ave	7.2222	21.2143	165.3352	288.651	2.1334	517.5541
QGWO	Std	12.8453	17.845	74.5621	74.5621	1.1321	77.1457
	p-value	0.0019	0.0045	0.0011	0.0019	0.0017	0.0025
	Ave	22.2143	68.2514	235.114	401.321	33.974	699.8142
QWOA	Std	23.3300	33.2514	56.9702	98.3524	33.974	88.46236
	p-value	0.0019	0.0035	0.0011	0.0019	0.0025	0.0022
	Ave	8.3625	15.0142	144.911	269.902	4.324	444.3251
SHADE	Std	8.1425	22.3333	3.1001	27.3333	1.531	65.7451
	p-value	0.0021	0.0044	0.0025	0.0023	0.0017	0.0044
	Ave	6.4521	14.0021	152.214	281.558	2.0906	396.8541
CMAES	Std	11.3322	22.1133	22.3324	45.3342	12.906	92.336
	p-value	0.0057	0.54	0.0033	0.0024	0.0022	0.0021
	Ave	6.3256	13.1935	151.6301	275.002	2.132	412.7133
LSHADE-SPACMA	Std	11.2211	24.1003	24.1003	27.3333	1.2341	77.556
	p-value	0.0033	0.0025	0.0033	0.0021	0.0022	0.0017

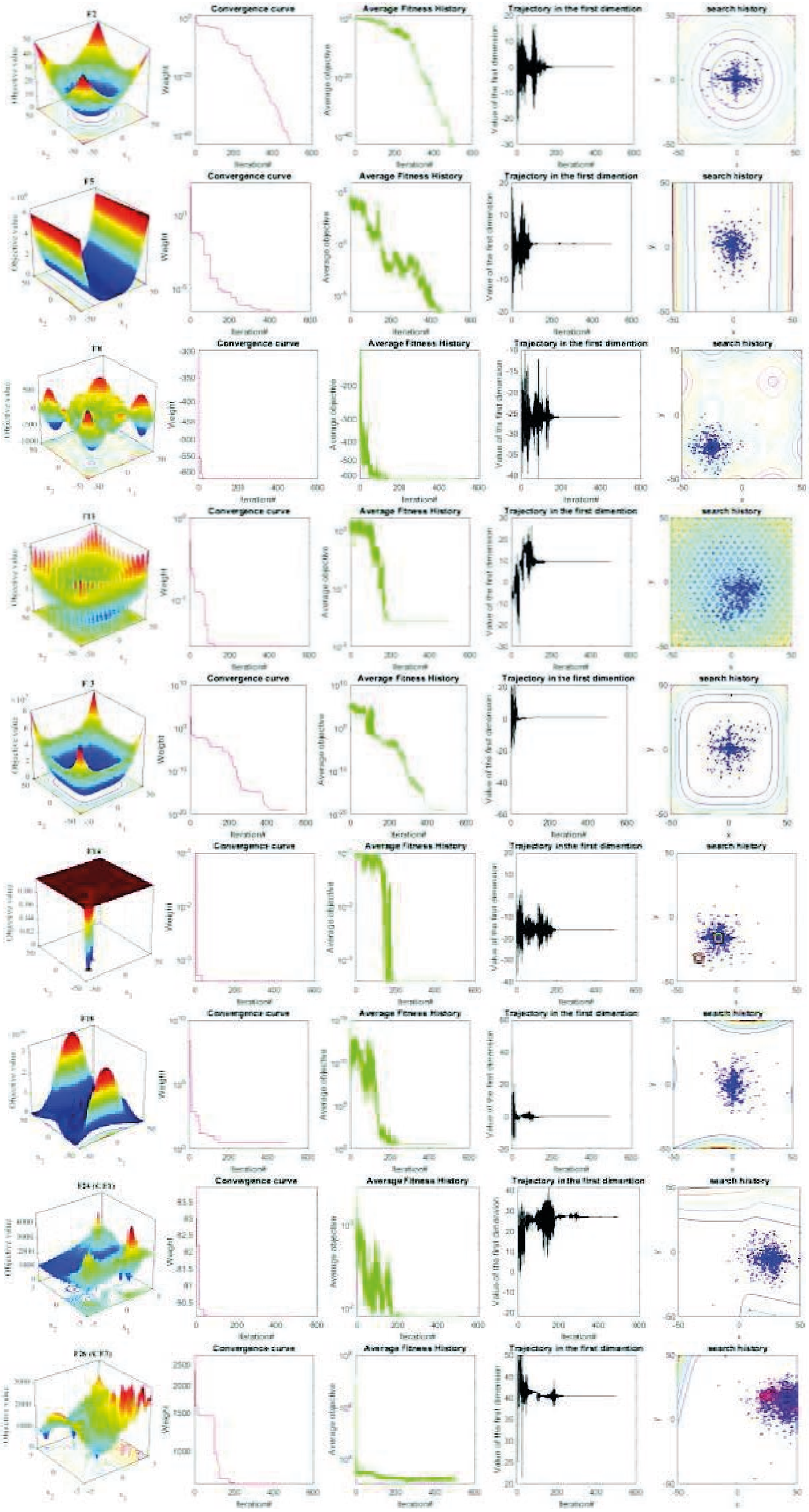

Figure 3. Search space, convergence curve, average fitness history, and first dimension's trajectory of some functions.

Table 11. Friedman mean rank statistics.

Algorithm	**ChOA**	**ULChOA**	**IChOA**	**NChOA**	**DLFChOA**	**QSA**
Friedman mean rank	11.29	5.8	10.94	10.075	8.87	6.87
Rank	12	6	11	10	9	7
Friedman mean rank	**QChOA**	**QGWO**	**QWOA**	**SHADE**	**CMAES**	**LSHADE-SPACMA**
Rank	2.14	4.36	8.59	3.65	2.68	5.82
	1	4	8	3	2	5

dicator to assess colony efficiency. The observed trend of the metric exhibits a resemblance to convergence rates, although it places particular emphasis on the enhancement of outcomes within the initial population resulting from this cooperative effort. The phase change of the algorithm results in an enhanced fitness level for each agent. The mean fitness history of test functions demonstrates a step-like pattern as a result of this improvement. Gradual and seamless changes generally characterize the gradients of the curves of UMs.

The skew patterns for these types are prominent in MM and CFs. A further measurement is the direction of the agents, which is illustrated in column 4. This metric provides an individual's topological changes from the optimization process's inception to its very end. The first dimension can represent the agents' route since they can go in numerous directions.

An algorithm is guaranteed to converge to the local minimum area in the end by following this pattern, which involves iteratively switching from an exploration-oriented to a local search-oriented strategy in later rounds. The changes in frequency, magnitude, and length of these phenomena are frequently more substantial compared to those of the UM functions. This is attributed to the distinct properties of MM and CFs, which exhibit a greater degree of radiculitis than UM functions.

Lastly, in the final column of the chart, we can see the results of searching history metric evaluation. Because of the agents' two-pronged reinforcement weighting behavior, QChOA is able to reveal patterns in their aggregate- seeking behavior in this image. In this model, UM functions more agents to occupy optimal points, but MM and CFs are more scattered in their search activity. Achieving success in UM endeavors is made more accessible by the central pattern's defining feature. Last but not least, we search the whole area by investigating the domain, which allows QChOA in MM and CFs. Furthermore, the convergence trajectory for particular assessment functions for the comparison algorithms is displayed in Figure 4.

Figure 4 shows the results of analyzing the QChOA and competitive approaches' convergence curves for optimization of the test functions. The findings show that phase one quickly approaches the global minimum, and phase two only makes marginal improvements over phase one, supporting the idea that only one stage may be effective in addressing a benchmark. This search pattern is visible in F1, F3, F4, and F11. Since the algorithm had already reached the optimal or nearly optimal state, we can observe another comparable pattern without enhancing solutions in the subsequent phases. F2, F16, F17, and TF18 all exhibit this pattern. Following each phase shift visible in F4, F8, F10, F26, and F28, the last pattern shows a modification in a convergence curve. Weight modification is employed by the QChOA in order to investigate and leverage the domain, hence enhancing the performance of the approach. Additionally, the fact that their convergence trajectories behave consistently across the last phase provides more evidence that these functions are converging.

A thorough comprehension of how weight changes affect algorithm performance as a whole can be achieved by including rigorous MM and CF. Additionally, these models elucidate the underlying reasoning behind the formulation of each phase. This approach allows QChOA to find the minima in the first phase of UM functions. The experimental effectiveness of each separate stage becomes evident and persuasive when the approach is evaluated in MMs and CFs.

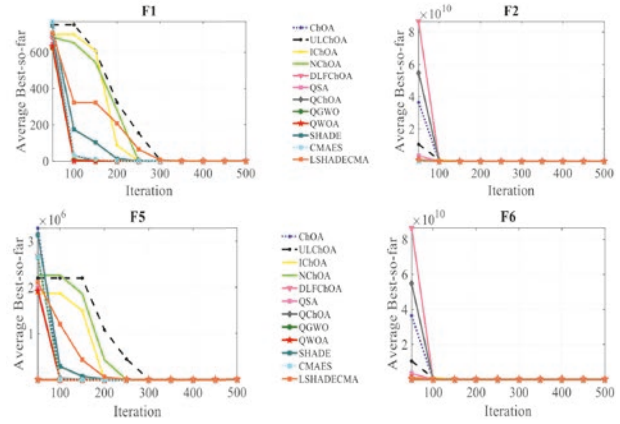

a) UM benchmark function

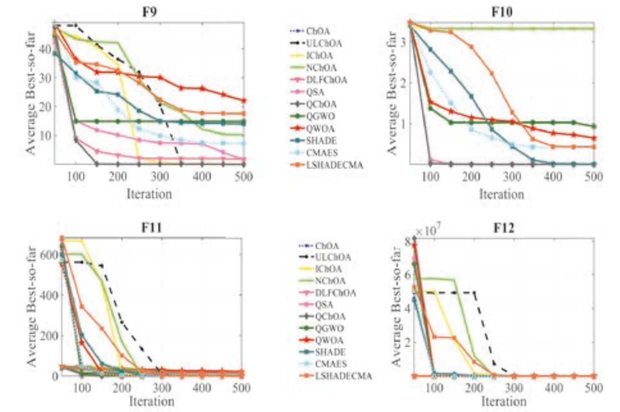

b) MM benchmark function

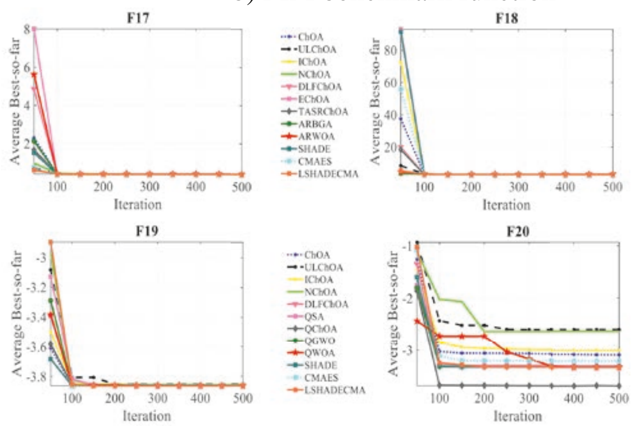

c) FDM benchmark function

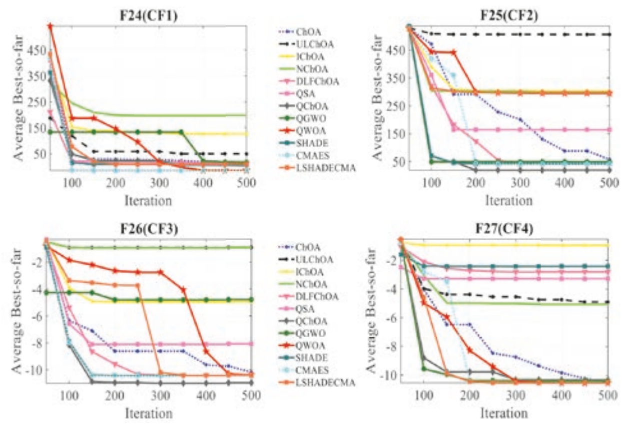

d) CFs

Figure 4. The convergence graphs of the QChOA and other benchmarks.

5.5 Performance of QChOA on CECBC2017 Test Functions

The study utilized the CECBC2017 test suite, which is recognized for its recentness and complexity, in order to evaluate numerical optimization contests [100]. This test suite has 30 functions, predominantly consisting of intricate hybrid and composite evaluation benchmark tasks. The purpose of employing this test suite is to demonstrate the performance of the suggested technique. Awad et al. [64] provided a comprehensive mathematical framework along with extensive details regarding this testbed. These functions are used to contrast the QChOA with other popular approaches. Table 12 displays the Ave, Std, and p-value. Numbers in bold represent the best performance achieved for each metric in each experiment.

According to Friedman's mean rank, QChOA and CMAES rank first and second. According to the findings, QChOA is the best of the existing optimizers.

5.6 Results of the IEEE CEC062019 100digit Challenge

In order to assess QChOA's performance even further, ten functions from the 100Digit Challenge CEC062019 [58] are used. Table A5 contains the functions' characteristics. In the IEEE CEC062019 100Digit competition, algorithms executed each test task 50 times. The minimal function evaluation counts the total accurate numbers across the 25 runs. The score of the test function is then computed using Nc/25. The optimal challenge score is 100 if at least 25 of 50 trials for every ten trials give ten-digit results. At least 1.000000000 must be achieved on tasks. A 3D representation of a few mentioned tasks is shown in Figure 5.

Figure 6 shows the results of 18 benchmark algorithms and standard ChOA and QChOA for each of the ten issues.

As shown in Figure 6, jDE100 yields the highest number of significant results with a score of 100, which DISHchain1e+12 follows. Out of twenty cutting-edge methods, the ChOA comes in at number six with an 87.6. Our method, which applies the QM to the ChOA, places third out of twenty benchmarking with a score of 94.11. It is important to note that the QChOA ranks highest in seven of the ten problems. However, because of the size of the challenges, QChOA has trouble with F5, F6, and F10 but does well with F7, F8, and F9. For 28 of the 35 test functions, the statistically best performance is achieved by QChOA. Notably, the QChOA performs better than the other cutting-edge benchmarks.

5.7 Statistical Analysis of QChOA

In this section, Bonferroni-Dunns and Holm and Friedman tests, are provided to compare the QChOA with its competitors. The functions were divided into three groups for the purpose of creating a trustworthy evaluation. All of the operations shown in Tables 7, 8, and 9 fall under the first group. In order to create the CFs, which are designated as F24–F29, several basic UM and MM functions are rotated, shifted, and mixed. The objective of producing the CFs is to assess the algorithms' capacity to effectively navigate away from local minima and strike a balance between exploration and exploitation. Table 10 presents the performance evaluation of various optimization methods in CFs, including the QChOA. The findings indicate that QChOA has a higher degree of overall effectiveness compared to alternative approaches. It appears from the results that the fine-tuned QChOA is quite good at balancing the two stages of its operation, exploitation and exploration. This leads to exceptional performance in avoiding local minima, which can be attributed to the complete relocation facilitated by QM. The benchmark algorithms' overall rank in this table is determined using Friedman's mean rank test. As seen by the data presented in Table 11, the QChOA algorithm demonstrated superior performance when compared to other baseline techniques.

Based on the data presented in Table 12, it can be observed that the CECBC2017 test functions constitute the second class. The third class is comprised of a synthesis of the first two classes. The statistical differentiation of the algorithms' performance can be achieved through the application of the nonparametric Friedman test. Upon detecting statistically significant changes in the performance of multiple algorithms, it is imperative to ascertain which algorithms exhibit a substantial deviation in efficiency compared to QChOA. As a result, to find out if there were any significant differences between

Table 12. Results for CECBC2017 benchmark functions

Type	No.	Metric	ChOA	ULChOA	IChOA	NChOA	DLFChOA	QSA
UM	F1	Ave	2741.28	274.33	9322.22	166.33	2433.22	417.88
		Std	345.21	274.31	5741.49	4.22E06	1952.112	362.74
		p-value	0.0033	0.0025	0.0044	0.0044	0.0033	0.0061
	F3	Ave	**300**	833.33	587.00	**300**	**300**	**300**
		Std	1.95E11	25.031	125.33	8.77E07	2.44E07	2.12E04
		p-value	**0.054**	0.0046	0.0055	0.0014	0.0033	0.0021
MM	F4	Ave	399.44	407.44	408.33	401.25	404.33	406.55
		Std	4.1425	7.652	2.22	1.4521	1.7412	1.4123
		p-value	0.0018	0.0017	0.0011	0.0033	0.0044	0.0027
	F5	Ave	511.77	509.21	512.55	509.33	509.33	508.22
		Std	2.4563	7.9654	4.6523	4.5412	4.4169	3.5551
		p-value	0.0033	0.0025	0.0044	0.0044	0.0033	0.0061
	F6	Ave	633.88	614.42	599.55	602.41	601.33	603.41
		Std	1.25E01	9.3332	1.44E02	5.11E04	1.02E04	2.3330
		p-value	0.0018	0.0017	0.0011	0.0033	0.0044	0.0027
	F7	Ave	722.33	714.33	719.55	720.10	720.10	717.33
		Std	4.4174	1.2336	5.3625	3.0333	5.3201	3.4141
		p-value	0.0014	0.07323	0.0024	0.0011	0.0036	0.0002
	F8	Ave	820.45	814.654	812.65	811.22	818.22	815.44
		Std	5.3333	2.4141	7.1523	2.3696	6.8585	5.9142
		p-value	0.0018	0.0017	0.0011	0.0033	0.0044	0.0027
	F9	Ave	902.36	**900.00**	**900.00**	905.33	**900.00**	902.11
		Std	5.33E14	**0.00**	5.98E14	0.0044	0.0512	1.1236
		p-value	0.0044	**0.143**	0.0024	0.0011	0.0036	0.0002
	F10	Ave	1652.11	1677.33	1633.11	1355.24	1411.33	2566.33
		Std	199.222	198.475	233.11	134.258	259.546	223.252
		p-value	0.0033	0.0025	0.0044	0.0044	0.0033	0.0061
Hybrid	F11	Ave	1117.25	1110.33	1106.25	1103.33	1105.42	1110.36
		Std	6.1425	7.5552	7.5533	2.33211	5.4414	9.3369
		p-value	0.0027	0.0017	0.0015	0.0033	0.0044	0.0027
	F12	Ave	1.38E+06	7.11E+05	3.55E+05	1.35E+03	1.03 E+05	1.81E+06
		Std	1.22E+06	4.22E+05	3.33E+05	6.76E+01	9.79 E+03	1.86E+06
		p-value	0.0024	0.0035	0.0044	0.0018	0.0019	0.0055
	F13	Ave	2.14E+03	1.4E+03	1.03E+04	1.31E+03	8.02E+03	9.85E+03
		Std	0.53E+03	25.3312	7.73E+03	7.33E+02	6.72E+03	2.14E+03
		p-value	0.0024	0.0011	0.0036	0.0002	0.0021	0.0046
	F14	Ave	7.47E+03	1.45E+03	1.45E+03	1.41E+03	1.46E+03	7.14E+03
		Std	8.15E+03	54.33	82.33	5.5221	31.54214	1.49E+03
		p-value	0.0018	0.0017	0.0011	0.0033	0.0044	0.0027
	F15	Ave	9.7E+03	1.62E+03	1.29E+03	1.50E+03	1.50E+03	2.23E+03
		Std	285.69	2.333	8.97	1.4421	1.3321	0.52E+03
		p-value	0.0031	0.0025	0.0044	0.0044	0.0033	0.0061
	F16	Ave	1.62E+03	1.64E+03	1.62E+03	1.60E+03	1.58E+03	1.82E+03
		Std	99.22	99.33	99.14	5.412	35.77	198.441
		p-value	0.0011	0.024	0.0036	0.0039	0.0014	0.0013
	F17	Ave	1.77E+03	1.75E+03	1.74E+03	1.73E+03	1.74E+03	1.77E+03
		Std	44.3321	29.1425	25.1245	6.4142	5.3365	27.2512
		p-value	0.0047	0.0002	0.0032	0.0021	0.0054	0.0061
	F18	Ave	1.85E+03	1.84E+03	1.83E+03	1.79E+03	1.83E+03	1.84E+03
		Std	45.3636	15.1414	45.2312	2.4758	17.3656	1.29E+04
		p-value	0.0024	0.0011	0.0036	0.0002	0.0021	0.0046
	F19	Ave	2.96E+03	2.91E+03	2.41E+03	1.91E+03	1.95E+03	1.94E+03
		Std	99.5454	74.1333	89.2552	1.1414	47.0021	41.3625
		p-value	0.0011	0.024	0.0036	0.0039	0.0014	0.0013
	F20	Ave	2.05E+03	2.03E+03	2.03E+03	2.01E+03	2.02E+03	2.27E+03
		Std	46.5521	7.1421	44.4747	5.02586	23.0231	82.0125
		p-value	0.0033	0.0025	0.0044	0.0044	0.0033	0.0061

CFs	F21	Ave	2.29E+03	2.21E+03	2.30E+03	**2.20E+03**	2.30E+03	2.28E+03
		Std	42.1625	39.1421	44.3333	**20.0202**	21.1475	39.6363
		p-value	0.0011	0.024	0.0036	**N/A**	0.0014	0.0013
	F22	Ave	2.30E+03	**2.03E+03**	2.29E+03	2.51E+03	2.29E+03	2.30E+03
		Std	13.4412	**12.2200**	19.3636	63.1425	17.1425	11.0120
		p-value	0.0017	**N/A**	0.0011	0.024	0.0036	0.0039
	F23	Ave	2.62E+03	2.61E+03	2.62E+03	2.61E+03	2.61E+03	2.72E+03
		Std	9.5554	10.3325	7.3321	8.1245	5.4141	233.321
		p-value	0.0011	0.0017	0.0036	0.0039	0.0014	0.0013
	F24	Ave	2.74E+03	2.74E+03	2.74E+03	2.56E+03	2.74E+03	2.73E+03
		Std	15.4412	5.4456	9.3321	42.4432	6.0021	64.0014
		p-value	0.0033	0.0025	0.0044	0.0044	0.0033	0.0061
	F25	Ave	2.95E+03	2.93E+03	2.94E+03	2.90E+03	2.93E+03	2.94E+03
		Std	248.1414	15.3311	20.07644	19.5541	19.5252	23.3636
		p-value	0.0024	0.0011	0.0036	0.0002	0.0021	0.0046
	F26	Ave	3.45E+03	3.44E+03	3.00E+03	2.90E+03	2.96E+03	2.92E+03
		Std	208.6541	632.7412	201.7474	25.3635	164.3321	32.3321
		p-value	0.0011	0.024	0.0025	0.0039	0.0033	0.0013
	F27	Ave	3.11E+03	3.11E+03	3.10E+03	3.09E+03	3.09E+03	3.09E+03
		Std	11.0021	14.3321	7.9963	8.9987	2.5598	2.5521
		p-value	0.0033	0.0025	0.0044	0.0044	0.0033	0.0061
	F28	Ave	3.31E+03	3.30E+03	3.31E+03	3.10E+03	3.30E+03	3.21E+03
		Std	156.332	90.142	112.444	19.8521	132.212	113.001
		p-value	0.0036	0.011	0.0036	0.0039	0.0014	0.0013
	F29	Ave	3.20E+03	3.20E+03	3.24E+03	3.15E+03	3.17E+03	3.21E+03
		Std	36.6666	44.9630	43.8520	13.4120	23.6654	51.3366
		p-value	0.0024	0.0011	0.0036	0.0002	0.0021	0.0046
	F30	Ave	5.31E+05	4.99E+05	4.63E+05	3.50E+03	3.01E+05	3.01E+05
		Std	4.89E+05	6.39E+05	4.92E+05	4.92E+03	4.52E+05	3.31E+05
		p-value	0.0033	0.0025	0.0044	0.0044	0.0033	0.0061
UM	F1	Ave	100.00	100.00	109.99	100	100	100
		Std	3.14E07	2.55E05	0.0021	0.000	0.000	4.33E06
		p-value	0.66	0.0041	0.0021	N/A	0.42	0.033
	F3	Ave	300.00	300.00	300.00	300.00	300.00	300.00
		Std	0.0000	9.94E11	1.25E03	0.000	0.000	1.11E33
		p-value	N/A	0.0011	0.0013	0.063	0.42	0.001
MM	F4	Ave	400.00	400.21	403.55	400.00	400.00	400.00
		Std	1.21E15	2.35E07	1.21E05	0.000	0.000	1.02E12
		p-value	0.056	0.0017	0.0043	N/A	0.052	0.0037
	F5	Ave	504.33	508.44	510.33	507.00	531.11	521.42
		Std	1.000	4.001	4.2222	1.007	59.11	56.19
		p-value	N/A	0.0011	0.0013	0.052	0.0033	0.0011
	F6	Ave	600.00	600.00	602.88	604.00	606.99	624.96
		Std	3.83E07	5.53E04	2.55E05	5.28E04	5.99E04	2.44E03
		p-value	N/A	0.0021	0.0033	0.0046	0.0011	0.0033
	F7	Ave	713.22	717.33	716.23	715.98	715.96	719.87
		Std	1.033	2.0014	1.0014	1.541	1.632	1.7112
		p-value	N/A	0.0021	0.0033	0.082	0.075	0.0033
	F8	Ave	805.64	806.33	807.71	806.85	806.84	810.93
		Std	1.845	2.5413	3.7831	1.8456	1.9863	2.1456
		p-value	N/A	0.0021	0.0033	0.082	0.075	0.0043
	F9	Ave	900.00	900.00	902.33	900.00	900.00	902.11
		Std	0.000	1.64E02	2.55E02	0.000	0.000	1.44E02
		p-value	N/A	0.0025	0.0037	0.056	0.053	0.0028
	F10	Ave	1189.38	1244.52	1355.33	1999.25	1195.26	1249.23
		Std	79.33	123.11	129.65	109.57	101.32	134.56
		p-value	N/A	0.0021	0.0033	0.0046	0.0011	0.0033

Hybrid	F11	Ave	1100.00	1102.01	1104.38	1102.56	1102.12	1104.11
		Std	0.96	1.44	2.11	1.32	1.31	2.77
		p-value	N/A	0.0077	0.0017	0.0018	0.082	0.0036
	F12	Ave	1323.55	1365.25	1411.12	1322.55	1323.20	1351.01
		Std	54.55	101.26	99.33	104.20	152.01	110.23
		p-value	0.21	0.0021	0.0021	N/A	0.0046	0.0011
	F13	Ave	1305.21	1305.31	1311.14	1306.77	1304.47	1309.25
		Std	3.22	2.89	3.33	2.71	0.69	2.51
		p-value	0.0021	0.0033	0.0046	0.0011	N/A	0.0011
	F14	Ave	1402.36	1404.22	1423.16	1409.82	1414.23	1449.38
		Std	4.01	4.09	7.33	8.63	9.22	10.99
		p-value	N/A	0.0023	0.0035	0.0046	0.0011	0.0033
	F15	Ave	1500.75	1500.76	1532	1501.33	1502.11	1554.06
		Std	0.53	0.53	1.11	0.59	057	2.11
		p-value	N/A	0.075	0.0025	0.082	0.056	0.0041
	F16	Ave	1601.01	1601.83	1614.23	1602.22	1603.25	1652.03
		Std	0.88	0.93	1.42	0.93	1.52	2.33
		p-value	N/A	0.0033	0.0017	0.0018	0.0072	0.0037
	F17	Ave	1705.15	1711.23	1717.88	1715.38	1711.78	1722.18
		Std	3.56	6.66	6.82	4.33	5.23	8.56
		p-value	N/A	0.0031	0.0017	0.0018	0.056	0.0029
	F18	Ave	1807.21	1808.33	1822.39	1811.25	1815.56	1844.23
		Std	4.21	5.22	6.89	6.44	7.12	9.56
		p-value	N/A	0.0071	0.0057	0.0058	0.0012	0.0047
	F19	Ave	1900.00	1902.11	1914.00	1902.14	1902.12	1905.33
		Std	0.00	1.22	2.14	1.33	1.23	3.55
		p-value	N/A	0.0027	0.0029	0.0041	0.0023	0.0033
	F20	Ave	2003.22	2004.45	2009.87	2005.33	2006.22	2011.22
		Std	0.69	1.33	2.11	1.22	1.25	2.33
		p-value	N/A	0.0033	0.0017	0.0018	0.082	0.0036

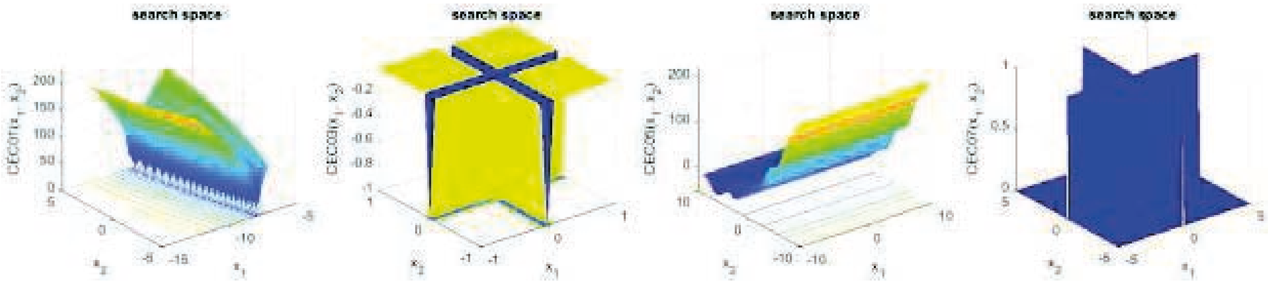

Figure 5. The three-dimension CEC062019 functions' search space.

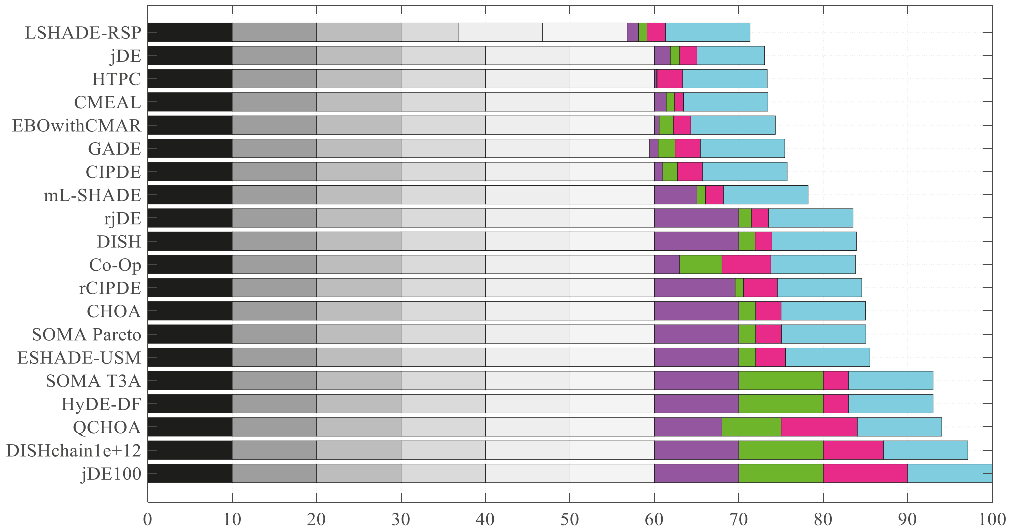

Figure 6. CEC062019 challenge results.

the two competitors, we used the Bonferroni-Dunn post hoc test, which uses the Critical Difference (CD) to quantify significance.

It should be mentioned that the control strategy in this experiment is QChOA. In Figure 7, we can see how each method fared on average over three different kinds of functions, with 0.1 and 0.05 being the significance levels for each. The QChOA algorithm can outperform algorithms that are ranked higher than the threshold line associated with the given figure. A colorcoded threshold line demarcates each category. Based on the graphical representation, QChOA demonstrates the highest ranking across all classes and exhibits the potential to significantly outperform alternative comparison algorithms at significance levels of both 0.1 and 0.05.

In conclusion, based on the findings presented in Figure 7, QChOA demonstrates strong and dependable performance in the specified functions when compared to existing optimizers. Across all three classes, there is a constant level of performance indicated by the marginal variance in the average ranking of QChOA. Nevertheless, certain strategies exhibit uneven ordering across different categories.

5.8 The Real-World Issues

Twelve problems from CEC2020, including industrial chemical process (heat exchanger network design (RC01) and reactor network design (RC04)), process design and synthesis (two-reactor problem (RC11) and multiproduct batch plant (RC14)), mechanical design problems (optimal design of industrial refrigeration system (RC16) and step cone pulley problem (RC23)), power system problems (optimal sizing of distributed generation for active power loss minimization (RC35) and optimal power flow (minimization of active power loss) (RC37)), power electronic problems (SOPWM for 3level inverters (RC45) and SOPWM for 11level Inverters (RC49)), livestock feed ration optimization (Beef Cattle (case 1) (RC51) and Beef Cattle (case 2) (RC52)) are applied to assess the QChOA's efficiency [88]. It is noteworthy to add that the comprehensive explanation of the suite test can be found in the CEC2020 publication by Kumar et al. [88]. The results are summarized in Table 13, as evidenced by the data presented.

In four particular issue instances—RC14, RC35, RC37, and RC39—the SHADE approach provides better performance than other techniques, as shown in Table 13. Additionally, the ULChOA method beats other techniques, specifically in issue instances RC23 and RC37. However, in the subsequent issues, it can be observed that the QChOA demonstrates the most optimal performance. Therefore, the statistical analysis reveals that the QChOA emerges as the most efficient approach for addressing real-world engineering challenges. In terms of the enhanced forms of ChOAs, the DLFChOA ranks second.

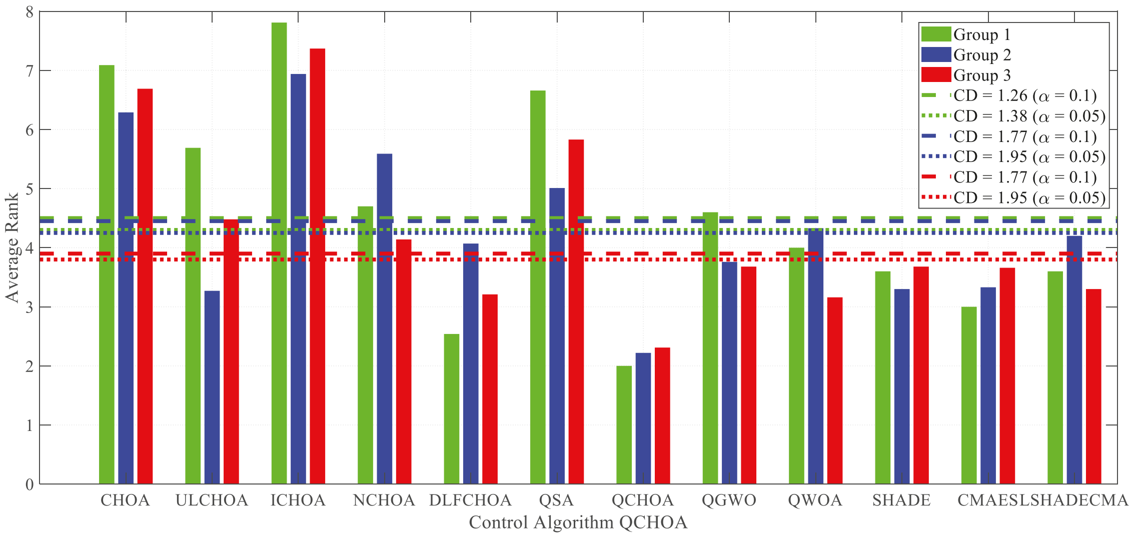

Figure 7. Bonferroni Dunn's test (0.05 and 0.1).

Table 13. The results of QChOA for CEC2020 problems (AVE±STD)

Algorithm	**ChOA**	**ULChOA**	**IChOA**	**NChOA**	**DLFChOA**	**QSA**
RC01	211±1.18	155±0.021	210±1.01	156±0.123	146±0.012	205±0.123
RC04	0.321±1.221	0.335±1.32	0.335±1.21	0.330±1.452	0.341±1.213	0.301±2.121
RC11	11.24±1.70	10.33±2.11	11.02±2.11	10.01 ±2.03	9.88±1.55	11.12±2.02
RC14	7220±3.21	6352±1.28	7330±2.11	6320±2.01	5963±1.12	6985±2.11
RC16	0.044±0.00021	0.046±0.00033	0.047±0.00022	0.043±0.00021	0.0042±0.00033	0.044±0.00036
RC23	30.00±4.31	25.12±2.32	31.13±5.42	25.13±4.01	23.01±2.01	30.22±4.11
RC35	0.0951±1.03	0.0963±0.532	0.0954±0.721	0.0942±0.623	0.0910±0.555	0.0944±1.01
RC37	0.0263±0.01	0.0233±0.015	0.0266±0.019	0.0225±0.014	**0.0221**±0.013	0.0244±0.019
RC45	0.0432±0.012	0.0425±0.0066	0.0425±0.011	0.0422±0.0053	0.0395±0.0012	0.0426±0.011
RC49	0.0511±0.086	0.0355±0.074	0.0485±0.082	0.0266±0.044	0.0238±0.015	0.0401±0.056
RC51	5030±2.33	4510±1.23	4999±2.36	4500±1.99	4995±1.23	5002±2.36
RC52	4010±311	3452±185	4009±302	3562±162	3385±152	3383±159
Algorithm	**QChOA**	**QGWO**	**QWOA**	**SHADE**	**CMAES**	**LSHADE-SPACMA**
RC01	**144±0.002**	155±0.021	173±0.632	144±0.021	145±0.120	145±0.025
RC04	**0.389**±1.02	0.366±1.25	0.352±1.45	0.388±1.03	0.385±1.44	0.385±1.11
RC11	**9.79**±**1.30**	10.22±2.12	11.44 ±2.01	9.88±1.45	9.89±1.32	9.98±1.78
RC14	5221±1.02	5362±2.01	5355±1.99	**5220 ±1.01**	5221±1.02	5222±1.11
RC16	**0.004±0.00016**	0.041±0.00022	0.041±0.00025	0.0042±0.00017	0.0041±0.00018	0.0041±0.00020
RC23	**22.4**±1.55	23.55±1.65	23.99±2.01	22.5±1.66	**22.4±1.41**	23.01±1.96
RC35	**0.0909±0.521**	0.0922±0.632	0.0932±0.655	**0.0909**±0.563	0.0910±0.533	0.0912±0.562
RC37	**0.0221±0.011**	0.0230±0.012	0.0228±0.012	**0.0221±0.011**	**0.0221±0.011**	0.0225±0.012
RC45	**0.0389±0.0010**	0.0401±0.0021	0.0401±0.0019	0.0392±0.0011	0.0393±0.0011	0.0396±0.0019
RC49	0.0235±0.011	0.0305±0.022	0.0300±0.018	**0.0227±0.010**	0.0228±0.011	0.0236±0.021
RC51	**4490±1.11**	4502±1.25	4500±1.23	4496±1.15	4492±1.12	4499±1.43
RC52	3392±175	3395±186	3394±175	3380±151	3386±160	3399±179

5.9 IEEE CEC 2022

Real-world optimization challenges often exhibit dynamically changing landscapes, whether it be in terms of the number of variables, objective function, and constraints. The author introduces the concept of dynamic optimization problems as a type of problem that undergoes evolution and necessitates real- time solutions using optimization techniques [95]. The discussion of addressing dynamic optimization problems requires algorithms that possess the ability to not only identify the most optimal solutions but also swiftly adapt to changes in the environment. This adaptability allows them to explore alternative solutions when previously identified ones are no longer optimal [95].

In order to conduct a comprehensive evaluation of QChOA and its ability to handle dynamic optimization problems, it is essential to have a suitable benchmark generator. In this particular field, the prevailing benchmark generators utilize a strategy that involves harnessing the power of various components to construct an optimization landscape meticulously. In the majority of the existing dynamic optimization problems benchmarks, the dynamic nature of characteristics such as height, width, and positioning of the elements mentioned above has been observed. Among these types of generators, the shifting peaks benchmark stands out. One thing that makes the rate of change, *cf* is the fitness assessment counter for every environment and the shifting peaks benchmark, a famous synthetic issue associated with dynamic optimization, stand out is that it uses only one peak to make all of its components.

However, it is worth noting that the classic moving peaks benchmark, although widely recognized, is characterized by landscapes that possess symmetric, smooth, regular, unimodal, and separable traits [8]. Consequently, these landscapes are generally straightforward to optimize. The characteristics mentioned above may not consistently reflect the complexities that are inherent in numerous real-life situations. In order to address this discrepancy, the authors of [1] have introduced a novel benchmark known as the generalized moving peaks benchmark. The generalized moving peaks benchmark provides the opportunity to generate components that exhibit a wide array of characteristics. These characteristics can range from straightforward, unimodal landscapes to intricate multimodal terrains. They can also include symmetrical forms as well as noticeable asymmetries.

Additionally, the generalized moving peaks benchmark allows for the creation of both smooth terrains and those that are filled with irregularities. Furthermore, it enables the exploration of various levels of variable interaction and condition numbers. The generalized moving peaks benchmark, renowned for its customizable features, offers an invaluable tool for scholars seeking to meticulously analyze the performance of dynamic optimization algorithms such as QChOA. By assessing their capabilities across a diverse range of problem attributes, researchers can gain profound insights into their effectiveness.

We use a primary performance metric to assess the effectiveness of algorithms on problem sets generated by generalized moving peaks benchmark: the offline error (OE) [96]. The calculation of OE is based on determining the average difference between the ideal position and all fitness evaluations, which is expressed by the following equation:

$$OE = \frac{1}{NE \times CF} \sum_{ne=1}^{NE} \sum_{cf=1}^{CF} \left(f^{ne}(BP^{ne}) - f^{ne}(BP^{(ne-1)CF+cf}) \right) \tag{20}$$

Where NE is the total number of such environments, $BP^n e$ denotes the best position in ne environment. Furthermore, CF denotes the rate of change, cf is the fitness assessment counter for every environment and $BP^{(t-1)CF+cf}$ corresponds to the top position at the cf_{th} fitness assessment in the ne_{th} environment.

Neutral or neutral and quantum individuals make up multi-swarms. Ω(M, M^q) is a simple way to express the multi-swarm arrangement, where M and M^q stand for the counts of quantum and neutral individuals in each swarm, respectively. Ω indicates the total number of swarms in the multi-swarm.

The following are the setup details unless otherwise noted: The five dimensions of the exploration domain are comprised of various peaks with randomly varying peak heights between [30, 70] and unpredictable peak width determinants between [1, 12]. Peaks relocate by a length in any direction after a predetermined number of assessments, and their transitions are independent. They were chosen to enable juxtaposition with the adaptive-scouts approach. After 100 peak transitions, each test ends, resulting in 500,000 function assessments.

Since a pseudorandom number generator controls the beginning point, initial amplitude, initial width, and future trajectory of the peaks, Scenario 1 effectively provides a suite of benchmark functions. Our findings are based on an average of fifty iterations, where each iteration uses an entirely distinct random seed for the optimization approach and a generalized moving peaks benchmark. The offline error [96], which calculates the mean discrepancy of the best solution found after the last environmental shift, is the primary effectiveness statistic used. This measure is always positive and goes to zero for perfect adaptation.

The investigation of the algorithm's responsiveness to certain parameter configurations is one of the main goals of the experimental series. Examining the effects of different multi-swarm architectures Ω(M, M^q) is another goal. The total ChOA count (aggregate population count) was limited to 100, with the exception of some instances, in order to align efficiency with the evolutionary approaches reported in [97]. Throughout all of our testing, we consistently used typical ChOA values mentioned in previous sections.

5.9.1 Implications of Different Multi-Swarm Setups

The first set of studies looks at how the multi-swarm configuration affects performance while using the generalized moving peaks benchmark and the previously specified standard settings.

There are numerous ways to put up 100 individuals. Swarm counts vary from 1 (multi-swarms merge into a single swarm ChOA and QChOA) to 100 (no more swarm essence as a single chimp cannot communicate with other chimps during updates). The optimal designs, mirroring the peak count, most likely lie in the middle of these two extremes. Symmetric configurations with 2–50 swarms, including the maximum and minimum, were tested wherever it was feasible. Nevertheless, there are no settings with an equal number of ChOA in every swarm for 11–19. Despite 14(4+3) having a total ChOA count of 98, the configuration was used to include a multi- swarm in this range.

Two sets of experiment results are presented: the severe circumstances (Ω=1 and Ω=100) and the overall results $\Omega \in [2:50]$.

- *Multiswarms:* First, multi-swarms with a visual representation in Figure 8, the effect of fluctuation on the offline error is recorded in Table 14. More swarms increase the diversity of the swarm. Data confirms our assumption that ten swarms is the optimal value for a parameter, showing that efficiency peaks at that number. Two reasons why adding more than ten swarms reduces the results are fewer chimps in more enormous swarms and redundant swarm peak ascension. The absence of charged swarm diversity causes results to drop, particularly in the conventional ChOA scenario with 50(1+1) small swarms. QChOA 10(5+5), on the other hand, works noticeably better. The constant outperformance of quantum interaction over charged interaction is interesting to see.
- *Extremum Setups*: Data for extreme setups with Ω=1 and Ω=100 are shown in Table 15. The single-swarm configurations confirm that the multi- swarm approach is practical. The slight variation between the 1(100+0) and 1(50+50) layouts is an unexpected finding. Large single populations are inherently diverse, and the moderate shift intensity of the generalized moving peaks benchmark does not undermine this. Swarm essence disappears because there is no way for inter-swarm communication to occur. Beyond the QChOA finding, it is evident that a single swarm that engages in localized information sharing performs better than Ω=100 that merely engages in exclusion-based interaction.

5.10 Computational Complexity Analysis

Suppose that y_m is a randomly distributed sequence; if for each $\varepsilon > 0 and \tau > 0, m_1(\varepsilon,\tau)$ can exist, the following equation will be satisfied:

$$\begin{gathered} Prob(|\gamma_m - s| < \varepsilon) > 1 - \tau \\ \forall m > m_1 or Prob(lim_{m\to\infty}|\gamma_m - s| < \varepsilon) \end{gathered} \tag{21}$$

The number of steps required to reach the ideal region $RG(\varepsilon)$ is used to measure the QChOA algorithm's performance. By contrasting the expected

Table 14. Various configurations (offline error ± standard error).

Configuration	**2(25+25)**	**3(17+16)**	**4(13+12)**	**5(10+10)**	**10(10+0)**	**10(0+10)**
CPSO	10.20±0.29	6.99±0.19	5.01±0.20	3.69±0.21	2.29±0.05	2.16±0.10
QPSO	9.80±0.41	6.69±0.30	4.80±0.20	3.68±0.20	2.29±0.05	1.89±0.07
ChOA	9.19±0.23	6.88±0.12	4.88±0.18	3.55±0.17	2.24±0.05	2.09±0.09
QChOA	8.77±0.31	6.73±0.11	4.68±0.14	3.44±0.14	2.23±0.04	1.86±0.06
Configuration	**10(5+5)**	**14(4+3)**	**20(3+2)**	**25(2+2)**	**50(1+1)**	
CPSO	1.99±0.05	2.30±0.08	2.90±0.08	3.30±0.10	15.40±0.39	
QPSO	1.69±0.05	1.89±0.05	2.40±0.08	2.70±0.06	4.01±0.11	
ChOA	1.88±0.04	2.22±0.06	2.85±0.07	3.11±0.07	14.22±0.28	
QChOA	1.42±0.03	1.73±0.04	2.32±0.06	2.41±0.05	3.97±0.09	

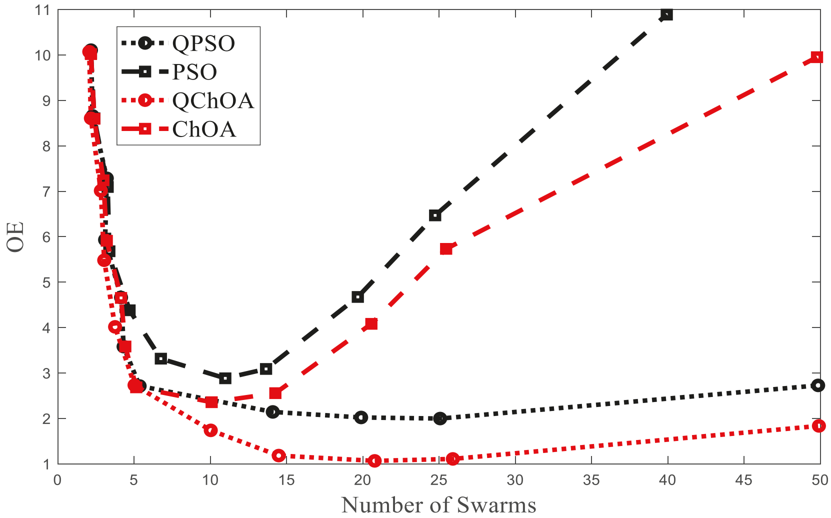

Figure 8. Number of swarms' influence on *OE* for 10(5 + 5) configuration.

Table 15. Extremum setups (offline error ± standard error.

Configuration	**1(100+0)**	**1(0+100)**	**1(50+50)**	**100(1+0)**	**100(0+1)**
CPSO	15.39±0.49	15.59±0.49	15.58±0.48	24.29±0.69	24.89±0.89
QPSO	15.39±0.49	15.79±0.49	15.09±0.48	24.29±0.69	14.29±0.11
ChOA	14.22±0.33	15.01±0.34	14.33±0.32	23.17±0.52	23.11±0.74
QChOA	14.22±0.32	15.09±0.34	14.01±0.11	23.11±0.51	8.09±0.02

value and distributional moments, the approach assesses the distribution of the number of steps required to reach $RG(\varepsilon)$. The maximum number of steps needed to get to the ideal region is given by

$$\mathrm{MNS}(\varepsilon) = \inf\{m \mid f_m \in RG(\varepsilon)\}$$

where inf denotes the infimum. The expectation value $\mathbb{E}(\mathrm{MNS}(\varepsilon))$ and the variance $\mathrm{Var}(\mathrm{MNS}(\varepsilon))$ are calculated as follows:

$$Exp(MNS(\varepsilon)) = \sum_{m=0}^{\infty} mz_m \tag{22}$$

$$\begin{aligned} Var(MNS(\varepsilon)) = \\ & Exp(MNS^2(\varepsilon)) - Exp(MNS(\varepsilon))^2 \\ & = \sum_{m=0}^{\infty} m^2 z_m - (\sum_{m=0}^{\infty} mz_m)^2 \end{aligned} \tag{23}$$

In practice, $\sum_{m=0}^{\infty} mz_m$ convergence is a prerequisite for $Exp(MNS(\varepsilon))$ to exist. $\sum_{i=0}^{m} z_i = 1$ is required for QChOA to converge globally. Time complexity is measured in terms of the number of objective function evaluations. The key advantage of this strategy is that it illustrates the link between CPU and measuring time as objective function complexity grows. We utilized the sphere function and a linear constraint to calculate the temporal complexity. Its lowest value is zero. The optimal region's value is set to $RG(\varepsilon) = RG(10^{-04})$. The algorithms ChOA and QChOA are run 40 times on f (z)with an initial scope of $[-10, 10]^{DIM} DIM$, the number of dimensions, to calculate the time complexity. We calculate the variance $Var(MNS(\varepsilon))$, the standard deviation (STD) $STD(MNS(\varepsilon))$, the standard error (SE)$\frac{STD(MNS(\varepsilon))}{\sqrt{40}}$, and the ratio of mean and dimension $\frac{MNS(\varepsilon)}{DIM}$. The statistical outcomes of the temporal complexity test for the QChOA and ChOA algorithms, respectively, are shown in Tables 16 and 17. Figure 9 shows that the suggested algorithm's temporal complexity increases nonlinearly as the dimension rises. However, the ChOA algorithm's time complexity increases appropriately linearly. As a result, QChOA has a lower temporal complexity than the ChOA algorithm.

$MNS(\varepsilon)$ and DIM are strongly correlated in Figure 9, according to QChOA, with a correlation coefficient of 0.9989. Compared to QChOA, ChOA's linear correlation coefficient, which stands at 0.9928, is not as astounding. Compared to the ChOA algorithm, the value of the correlation coefficient for QChOA is more stable, as evidenced by the correlation between mean and dimension.

5.11 Detailed Analysis of Experimental Results

This subsection will explore the fundamental technological principles that enable the QChOA algorithm to attain superior optimization performance compared to other contemporary algorithms.

5.11.1 Quantum-Inspired Superposition and Measurement

The QChOA algorithm utilizes quantum- inspired operators, including superposition and measurement, to facilitate practical exploration and exploitation of the solution space. The principle of superposition enables Quantum computing and QChOA to explore a diverse

The above attribute significantly augments the algorithm's capacity to examine various regions inside the search space concurrently. The measurement process guides the algorithm to select solutions with higher fitness values probabilistically, directing it toward promising areas.

The dual-process approach can be analogized to studying a "parallel universe," wherein the algorithm simultaneously traverses numerous alternative solution routes. Utilizing a quantum-inspired methodology facilitates the mitigation of local optima by enabling the algorithm to encompass a broader spectrum of options during each iteration.

5.11.2 Chaotic Dynamics for Enhanced Exploration

The use of chaotic dynamics, facilitated by adaptive chaotic search, introduces a controlled element of randomness to the optimization procedure. Chaotic maps, such as the logistic map or the tent map, incorporate non-linearity and stochasticity into the trajectory of the search process. This phenomenon proves particularly advantageous in scenarios where conventional optimization algorithms may have difficulties escaping local optima due to their deterministic nature.

Table 16. The statistical outcomes of the time complexity for the QChOA

DIM	$MNS(\varepsilon)$	$Var(MNS(\varepsilon))$	$STD(MNS(\varepsilon))$	SE	$\frac{MNS(}{DIM}$
2	299.25	4158.11	64.48	10.20	149.63
3	449.02	4499.12	67.07	10.61	149.67
4	619.11	4985.32	70.60	11.17	154.77
5	742.55	6532.22	80.82	12.78	148.51
6	868.05	8225.36	90.69	14.32	144.67
7	1011.11	8952.21	94.61	14.97	144.44
8	1144.44	9012.32	94.93	15.02	143.05
9	1288.52	10236.25	101.17	16.00	143.16
10	1440.25	11325.44	106.41	16.83	144.03

Table 17. The statistical outcomes of the time complexity for the standard ChOA

DIM	$MNS(\varepsilon)$	$Var(MNS(\varepsilon))$	$STD(MNS(\varepsilon))$	$\frac{STD(MNS(\varepsilon))}{\sqrt{40}}$	$\frac{MNS(\varepsilon)}{\text{DIM}}$
2	689.32	16524.21	128.54	20.33	344.66
3	968.21	20325.28	142.24	22.50	322.73
4	1159.24	22541.25	150.14	23.76	289.81
5	1198.36	20145.19	141.93	22.45	239.67
6	1244.52	29215.96	170.92	27.04	207.42
7	1365.21	48941.85	221.22	35.00	195.03
8	1529.24	42158.96	205.32	32.48	191.15
9	1752.25	38174.64	195.38	30.91	194.69
10	2452.32	41754.15	204.33	32.33	245.23

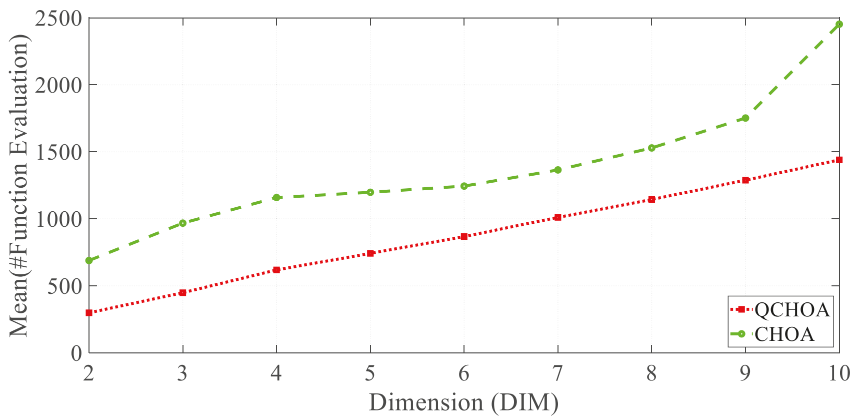

Figure 9. $MNS(\varepsilon)$ vs. DIM

Including a chaotic component in the search process enhances diversification, mitigating the risk of premature convergence to unsatisfactory answers by the algorithm. The QChOA method incorporates a deliberate degree of randomness in the search process, enabling it to overcome suboptimal solutions that may arise from local search and venture into unexplored regions of the search space.

5.11.3 Exploitation-Exploration Trade-off

One of the primary issues encountered in optimization involves effectively managing the trade-off between exploitation and exploration. The quantum operators and chaotic dynamics employed by QChOA synergistically collaborate to attain a state of equilibrium. The presence of a chaotic component in the algorithm promotes the exploration of different locations. At the same time, the utilization of quantum operators guides the algorithm towards promising regions characterized by higher fitness values.

The superposition and measurement operators influence the dynamic balance between exploration and exploitation. The probability of selecting solutions with high fitness values increases, successfully directing the algorithm toward convergence. Nevertheless, the inherent quantum properties of the algorithm guarantee that a broad range of potential solutions are taken into account, preventing early convergence towards poor solutions.

5.11.4 Sensitivity to Problem Characteristics

The versatility of the QChOA algorithm can be attributed to its ability to effectively respond to problem features, which is achieved through an adaptive chaotic mechanism. Various optimization problems exhibit distinct landscapes, and the flexibility of QChOA enables it to customize its behavior to address individual issues. The method's adaptability is accomplished by dynamically adjusting the parameters of the chaotic map, which allows for finetuning the exploration-exploitation balance in response to the complexities inherent in the challenge at hand.

5.11.5 Analysis of Convergence Behavior

Figures 3 and 4 depict the convergence behavior of QChOA across iterations on specific benchmark tasks. The method converges quickly towards ideal or very close to optimal solutions. The observed behavior can be ascribed to the complimentary interplay of quantum operators and chaotic dynamics. The utilization of quantum-inspired exploration expedites the initial convergence process. At the same time, chaotic dynamics guarantee that the QChOA consistently explores various regions to enhance and refine the solutions.

5.11.6 Algorithmic Robustness and Parameter Sensitivity

One notable attribute of QChOA is its resilience when confronted with diverse parameter configurations. By conducting sensitivity analysis, it was revealed that the algorithm consistently produces competitive outcomes across various parameter values. The algorithm's reliability and effectiveness are further emphasized by its robustness, rendering it well-suited for a diverse range of optimization issues.

In conclusion, the QChOA algorithm demonstrates excellent performance due to its complex technical processes. The algorithm's performance in exploring and exploiting solution spaces, as well as adapting to the specifics of each problem, is improved by including quantum-inspired agents and chaotic dynamics. The QChOA method possesses a notable level of technical depth and adaptability, which enables it to surpass other algorithms in its performance across a wide range of real-world engineering optimization challenges.

6 Conclusion

In this study, QChOA, quantum-based ChOA, was developed to address the main drawbacks of the original approach, which include slow convergence and the tendency to reach local optimums when dealing with multidimensional problems efficiently. In order to address the two mentioned research gaps, this proposed technique incorporated two innovative approaches into the original ChOA. The quantum mechanism was used to increase the convergence rate of this algorithm. In addition, it was developed to enhance early trends in exploration search and late trends in exploitation. The algorithm's total search ability and convergence speed were both greatly enhanced by combining the two techniques. Twentynine conventional optimization test functions, thirty complicated CECBC functions, ten functions of the CEC06 test suit, ten real-world, application-based engineering challenges, and IEEE CEC 2022 competition on dynamic optimization problems were used to conduct in-depth analyses of the merits of the proposed QChOA. The QChOA was tested via four categories of optimization techniques, including (1) DLFChOA, ULChOA, NCHOA, IChOA as novel variants of ChOA, (2) QGWO, QSA, and QWOA as the three best quantum-behaved variant optimization algorithms, (3) SHADE, CMAES, and LSHADE-SPACMA as the three state-of-theart optimization algorithms, and 18 well-known algorithms in IEEE CEC competitions. A comprehensive evaluation was carried out using three nonparametric statistical tests: Wilcoxon rank-sum, Holm– Bonferroni, and Friedman average rank tests. The findings revealed that the QChOA ranked top among 51 out of 70 test functions and engineering challenges and displayed comparable outcomes to SHADE and CMAES in other comparisons. The analytical research showed that QChOA is statistically identical to jDE100 and DISHchain1e+12 while being a much better optimizer than the benchmark algorithms for the three first categories.

The exploring capabilities of the QChOA should be enhanced by using different chaotic maps. Because the weighted models were chosen through tests, mathematically validating the optimal weighted coefficient might constitute another subject for future research. It would also be beneficial to create a binary version of QChOA that has several objectives.

Declaration

Conflicts of interest/ Competing interests The authors declare that there is no conflict of interest

Data availibity

The data can be shared upon a reasonable request.

Funding Statement

This research was conducted without external funding. All aspects of the study, including data collection, analysis, and manuscript

preparation, were carried out by the authors voluntarily, without financial support from any funding agency or organization.

References

[1] C. Wang, Y. Wang, K. Wang, Y. Dong, and Y. Yang, An Improved Hybrid Algorithm Based on Biogeography/Complex and Metropolis for Many-Objective Optimization, Math. Probl. Eng., vol. 2017, no. 1, p. 2462891, 2017.

[2] F. Yu, C. Lu, J. Zhou, L. Yin, and K. Wang, A knowledge-guided bi- population evolutionary algorithm for energy-efficient scheduling of distributed flexible job shop problem, Eng. Appl. Artif. Intell., vol. 128, p. 107458, 2024.

[3] K. Liu et al., Research on fault diagnosis method of vehicle cable terminal based on time series segmentation for graph neural network model, Measurement, p. 114999, 2024.

[4] C. Wang, Z. Wang, S. Zhang, X. Liu, and J. Tan, Reinforced quantum- behaved particle swarm-optimized neural network for cross-sectional distortion prediction of novel variable- diameter-die-formed metal bent tubes, J. Comput. Des. Eng., vol. 10, no. 3, pp. 1060–1079, 2023.

[5] W. Liu, X. Bai, H. Yang, R. Bao, and J. Liu, Tendon driven bistable origami flexible gripper for high-speed adaptive grasping, IEEE Robot. Autom. Lett., 2024.

[6] W. Dang et al., Increasing Text Filtering Accuracy with Improved LSTM, Comput. Informatics, vol. 42, no. 6, pp. 1491–1517, 2023.

[7] B. Cao, Y. Gu, Z. Lv, S. Yang, J. Zhao, and Y. Li, RFID Reader Anticollision Based on Distributed Parallel Particle Swarm Optimization, IEEE Internet Things J., vol. 8, no. 5, pp. 3099–3107, 2020.

[8] R. Wang and R. Zhang, Techno- economic analysis and optimization of hybrid energy systems based on hydrogen storage for sustainable energy utilization by a biological-inspired optimization algorithm, J. Energy Storage, vol. 66, p. 107469, 2023.

[9] H. Jia, S. Shi, D. Wu, H. Rao, J. Zhang, and L. Abualigah, Improve coati optimization algorithm for solving constrained engineering optimization problems, J. Comput. Des. Eng., vol. 10, no. 6, pp. 2223–2250, 2023.

[10] L. Yin, M. Zhuang, J. Jia, and H. Wang, Energy saving in flow-shop scheduling management: an improved multiobjective model based on grey wolf optimization algorithm, Math. Probl. Eng., vol. 2020, pp. 1–14, 2020.

[11] R. Luo, Z. Peng, J. Hu, and B. K. Ghosh, Adaptive optimal control of affine nonlinear systems via identifier– critic neural network approximation with relaxed PE conditions, Neural Networks, vol. 167, pp. 588–600, 2023.

[12] M. Shi, W. Hu, M. Li, J. Zhang, X. Song, and W. Sun, Ensemble regression based on polynomial regression-based decision tree and its application in the in-situ data of tunnel boring machine, Mech. Syst. Signal Process., vol. 188, p. 110022, 2023.

[13] G. Arun and V. Mishra, A review on quantum computing and communication, in 2014 2nd International Conference on Emerging Technology Trends in Electronics, Communication and Networking, IEEE, 2014, pp. 1–5.

[14] R. P. Feynman, Simulating physics with computers, in Feynman and computation, CRC Press, 2018, pp. 133–153.

[15] S. Ramlo, Mixed methods research and quantum theory: Q methodology as an exemplar for complementarity, J. Mix. Methods Res., vol. 16, no. 2, pp. 226–241, 2022.

[16] D. Deutsch and R. Jozsa, Rapid solution of problems by quantum computation, Proc. R. Soc. London. Ser. A Math. Phys. Sci., vol. 439, no. 1907, pp. 553–558, 1992.

[17] M. Cerezo et al., Variational quantum algorithms, Nat. Rev. Phys., vol. 3, no. 9, pp. 625–644, 2021.

[18] P. W. Shor, Algorithms for quantum computation: discrete logarithms and factoring, in Proceedings 35th annual symposium on foundations of computer science, Ieee, 1994, pp. 124–134.

[19] X. Li and Y. Sun, Application of RBF neural network optimal segmentation algorithm in credit rating, Neural Comput. Appl., vol. 33, pp. 8227–8235, 2021.

[20] L. Luan, Z. Wang, and S. Liu, Progress of grover quantum search algorithm, Energy Procedia, vol. 16, pp. 1701–1706, 2012.

[21] L. Zhu et al., Adaptive quantum approximate optimization algorithm for solving combinatorial problems on a quantum computer, Phys. Rev. Res., vol. 4, no. 3, p. 33029, 2022.

[22] X. Xu and Z. Wei, Dynamic pickup and delivery problem with transshipments and LIFO constraints, Comput. Ind. Eng., vol. 175, p. 108835, 2023.

[23] B. Cao et al., Multiobjective 3-D topology optimization of next- generation wireless data center network, IEEE Trans. Ind. Informatics, vol. 16, no. 5, pp. 3597– 3605, 2019.

[24] B. S. Yıldız, N. Pholdee, N. Panagant, S. Bureerat, A. R. Yildiz, and S. M. Sait, A novel chaotic Henry gas solubility optimization algorithm for solving real-world engineering problems, Eng. Comput., pp. 1–13, 2021.

[25] B. S. Yıldız, S. Kumar, N. Pholdee, S. Bureerat, S. M. Sait, and A. R. Yildiz, A new chaotic Lévy flight distribution optimization algorithm for solving constrained engineering problems, Expert Syst., vol. 39, no. 8, p. e12992, 2022.

[26] D. Gürses, P. Mehta, S. M. Sait, and A. R. Yildiz, African vultures optimization algorithm for optimization of shell and tube heat exchangers, Mater. Test., vol. 64, no. 8, pp. 1234– 1241, 2022.

[27] D. Gürses, P. Mehta, V. Patel, S. M. Sait, and A. R. Yildiz, Artificial gorilla troops algorithm for the optimization of a fine plate heat exchanger, Mater. Test., vol. 64, no. 9, pp. 1325–1331, 2022.

[28] P. Mehta, B. S. Yildiz, S. M. Sait, and A. R. Yildiz, Hunger games search algorithm for global optimization of engineering design problems, Mater. Test., vol. 64, no. 4, pp. 524–532, 2022.

[29] A. Alazeb et al., Remote intelligent perception system for multi-object detection, Front. Neurorobot., vol. 18, p. 1398703, 2024.

[30] Y. Hartmann, H. Liu, and T. Schultz, High-level features for human activity recognition and modeling, in International Joint Conference on Biomedical Engineering Systems and Technologies, Springer, 2022, pp. 141– 163.

[31] L. S. Madsen et al., Quantum computational advantage with a programmable photonic processor, Nature, vol. 606, no. 7912, pp. 75–81, 2022.

[32] X. Cai et al., An improved quantum- inspired cooperative co-evolution algorithm with muli-strategy and its application, Expert Syst. Appl., vol. 171, p. 114629, 2021.

[33] W. Ding and J. Wang, A novel approach to minimum attribute reduction based on quantum-inspired self-adaptive cooperative co-evolution, Knowledge-Based Syst., vol. 50, pp. 1– 13, 2013.

[34] C. Yu, A. A. Heidari, and H. Chen, A quantum-behaved simulated annealing algorithm-based moth-flame optimization method, Appl. Math. Model., vol. 87, pp. 1–19, 2020.

[35] R. K. Agrawal, B. Kaur, and S. Sharma, Quantum based whale optimization algorithm for wrapper feature selection, Appl. Soft Comput., vol. 89, p. 106092, 2020.

[36] Y. Chen, F. Li, J. Wang, B. Tang, and X. Zhou, Quantum recurrent encoder– decoder neural network for performance trend prediction of rotating machinery, Knowledge-Based Syst., vol. 197, p. 105863, 2020.

[37] J. Chen, X. Qi, L. Chen, F. Chen, and G. Cheng, Quantum-inspired ant lion optimized hybrid k-means for cluster analysis and intrusion detection, Knowledge-Based Syst., vol. 203, p. 106167, 2020.

[38] R. V Casaña-Eslava, P. J. G. Lisboa, S. Ortega-Martorell, I. H. Jarman, and J. D. Martín-Guerrero, Probabilistic quantum clustering, Knowledge-Based Syst., vol. 194, p. 105567, 2020.

[39] P. Yan, L. Li, and D. Zeng, Quantum Probability-inspired Graph Attention Network for Modeling Complex Text Interaction, Knowledge-Based Syst., vol. 234, p. 107557, 2021.

[40] W. Deng et al., Quantum differential evolution with cooperative coevolution framework and hybrid mutation strategy for large scale optimization, Knowledge-Based Syst., vol. 224, p. 107080, 2021.

[41] M. Sharma, S. Gupta, H. Aggarwal, T. Aggarwal, D. Gupta, and A. Khanna, Quantum Grey Wolf optimisation and evolutionary algorithms for diagnosis of Alzheimer's disease, Int. J. Model. Identif. Control, vol. 41, no. 1–2, pp. 53–67, 2022.

[42] N.-R. Zhou, S.-H. Xia, Y. Ma, and Y. Zhang, Quantum particle swarm optimization algorithm with the truncated mean stabilization strategy, Quantum Inf. Process., vol. 21, no. 2, pp. 1–23, 2022.

[43] T. Liu, L. Jiao, W. Ma, J. Ma, and R. Shang, A new quantum-behaved particle swarm optimization based on cultural evolution mechanism for multi-objective problems, Knowledge- Based Syst., vol. 101, pp. 90–99, 2016.

[44] A. M. Anter, H. S. Elnashar, and Z. Zhang, QMVO-SCDL: A new regression model for fMRI pain decoding using quantum-behaved sparse dictionary learning, Knowledge-Based Syst., vol. 252, p. 109323, 2022.

[45] S. Yarkoni, E. Raponi, T. Bäck, and S. Schmitt, Quantum annealing for industry applications: Introduction and review, Reports Prog. Phys., 2022.

[46] J. Li, B. Xu, Y. Yang, and H. Wu, Quantum ant colony optimization algorithm for AGVs path planning based on Bloch coordinates of pheromones, Nat. Comput., vol. 19, pp. 673–682, 2020.

[47] M. Khishe and M. R. Mosavi, Chimp optimization algorithm, Expert Syst. Appl., 2020, doi: 10.1016/j.eswa.2020.113338.

[48] T. Hu, M. Khishe, M. Mohammadi, G.-R. Parvizi, S. H. T. Karim, and T. A. Rashid, Real-time COVID-19 diagnosis from X-Ray images using deep CNN and extreme learning machines stabilized by chimp optimization algorithm, Biomed. Signal Process. Control, p. 102764, 2021.

[49] A. N. Ahmed, T. Van Lam, N. D. Hung, N. Van Thieu, O. Kisi, and A. El-Shafie, A comprehensive comparison of recent developed meta- heuristic algorithms for streamflow time series forecasting problem, Appl. Soft Comput., vol. 105, p. 107282, 2021.

[50] E. H. Houssein, M. M. Emam, and A. Ali, An efficient multilevel thresholding segmentation method for thermography breast cancer imaging based on improved chimp optimization algorithm, Expert Syst. Appl., p. 115651, 2021, doi: https://doi.org/10.1016/j.eswa.2021.115 651.

[51] Y. Tang, S. Liu, Y. Deng, Y. Zhang, L. Yin, and W. Zheng, Construction of force haptic reappearance system based on Geomagic Touch haptic device, Comput. Methods Programs Biomed., vol. 190, p. 105344, 2020.

[52] D. Wu, W. Zhang, H. Jia, and X. Leng, Simultaneous feature selection and support vector machine optimization using an enhanced chimp optimization algorithm, Algorithms, vol. 14, no. 10, p. 282, 2021.

[53] F. Valdez, O. Castillo, and P. Melin, An Exhaustive Review of Bio-Inspired Algorithms and its Applications for Optimization in Fuzzy Clustering, 2021.

[54] S. P. H. Boroujeni and E. Pashaei, Data clustering using chimp optimization algorithm, in 2021 11th international conference on computer engineering and knowledge (ICCKE), IEEE, 2021, pp. 296–301.

[55] L. Zhu, H. Ren, M. Habibi, K. J. Mohammed, and M. A. Khadimallah, Predicting the environmental economic dispatch problem for reducing waste nonrenewable materials via an innovative constraint multi- objective Chimp Optimization Algorithm, J. Clean. Prod., vol. 365, p. 132697, 2022.

[56] T. Sui, D. Marelli, X. Sun, and M. Fu, Multi-sensor state estimation over lossy channels using coded measurements, Automatica, vol. 111, p. 108561, 2020.

[57] X. Xu, C. Wang, and P. Zhou, GVRP considered oil-gas recovery in refined oil distribution: from an environmental perspective, Int. J. Prod. Econ., vol. 235, p. 108078, 2021.

[58] L. Ding et al., Definition and application of variable resistance coefficient for wheeled mobile robots on deformable terrain, IEEE Trans. Robot., vol. 36, no. 3, pp. 894–909, 2020.

[59] M. Khishe and M. R. Mosavi, Classification of underwater acoustical dataset using neural network trained by Chimp Optimization Algorithm, Appl. Acoust., 2020, doi: 10.1016/j.apacoust.2019.107005.

[60] A. Fathy, D. Yousri, A. Y. Abdelaziz, and H. S. Ramadan, Robust approach based chimp optimization algorithm for minimizing power loss of electrical distribution networks via allocating distributed generators, Sustain. Energy Technol. Assessments, vol. 47, p. 101359, 2021.

[61] S. Bhattacharya, S. L. Tripathi, and V. K. Kamboj, Design of tunnel FET architectures for low power application using improved Chimp optimizer algorithm, Eng. Comput., pp. 1–44, 2021.

[62] N. Du, Q. Luo, Y. Du, and Y. Zhou, Color Image Enhancement: A Metaheuristic Chimp Optimization Algorithm, Neural Process. Lett., pp. 1–40, 2022.

[63] Z. Chen, K. Zhang, T. H. T. Chan, X. Li, and S. Zhao, A Novel Hybrid Whale-Chimp Optimization Algorithm for Structural Damage Detection, Appl. Sci., vol. 12, no. 18, p. 9036, 2022.

[64] Y. Yang, Y. Wu, H. Yuan, M. Khishe, and M. Mohammadi, Nodes Clustering and Multi-Hop Routing Protocol Optimization using Hybrid Chimp Optimization and Hunger Games Search Algorithms for Sustainable Energy Efficient Underwater Wireless Sensor Networks, Sustain. Comput.Informatics Syst., p. 100731, 2022.

[65] M. Kaur, R. Kaur, and N. Singh, A novel hybrid of chimp with cuckoo search algorithm for the optimal designing of digital infinite impulse response filter using high-level synthesis, Soft Comput., pp. 1–25, 2022.

[66] M. Kaur, R. Kaur, N. Singh, and G. Dhiman, SChoA: an newly fusion of sine and cosine with chimp optimization algorithm for HLS of datapaths in digital filters and engineering applications, Eng. Comput., 2021, doi: 10.1007/s00366- 020-01233-2.

[67] O. A. M. F. Alnaggar, B. N. Jagadale, and S. H. Narayan, MRI Brain Tumor Detection Using Boosted Crossbred Random Forests and Chimp Optimization Algorithm Based Convolutional Neural Networks .

[68] M. E. Zayed et al., Predicting the performance of solar dish Stirling power plant using a hybrid random vector functional link/chimp optimization model, Sol. Energy, vol. 222, pp. 1–17, 2021.

[69] F. Mousavipour and M. R. Mosavi, Sonar Data Classification using Neural Network Trained by Hybrid Dragonfly and Chimp Optimization Algorithms, 2022.

[70] G. Dhiman, SSC: A hybrid nature- inspired metaheuristic optimization algorithm for engineering applications, Knowledge-Based Syst., vol. 222, p. 106926, 2021.

[71] A. Saffari, S. H. Zahiri, M. Khishe, and seyyed mohammadreza mosavi, Design of a fuzzy model of control parameters of chimp algorithm optimization for automatic sonar targets recognition, IJMT, 2020, [Online]. Available: http://ijmt.iranjournals.ir/article_24112 6.html

[72] H. Jia, K. Sun, W. Zhang, and X. Leng, An enhanced chimp optimization algorithm for continuous optimization domains, Complex Intell. Syst., pp. 1– 18, 2021.

[73] M. Khishe, M. Nezhadshahbodaghi, M. R. Mosavi, and D. Martín, A Weighted Chimp Optimization Algorithm, IEEE Access, 2021.

[74] W. Kaidi, M. Khishe, and M. Mohammadi, Dynamic Levy Flight Chimp Optimization, Knowledge- Based Syst., p. 107625, 2021.

[75] G. Hu, W. Dou, X. Wang, and M. Abbas, An enhanced chimp optimization algorithm for optimal degree reduction of Said–Ball curves, Math. Comput. Simul., vol. 197, pp. 207–252, 2022.

[76] Q. Zhang, S. Du, Y. Zhang, H. Wu, K. Duan, and Y. Lin, A Novel Chimp Optimization Algorithm with Refraction Learning and Its Engineering Applications, Algorithms, vol. 15, no. 6, p. 189, 2022.

[77] N. Du, Y. Zhou, W. Deng, and Q. Luo, Improved chimp optimization algorithm for three-dimensional path planning problem, Multimed. Tools Appl., pp. 1–26, 2022.

[78] N. Du, Y. Zhou, Q. Luo, M. Jiang, and W. Deng, Multi-strategy chimp optimization algorithm for global optimization and minimum spanning tree, Soft Comput., pp. 1–28, 2023.

[79] D. H. Wolpert and W. G. Macready, No free lunch theorems for optimization, IEEE Trans. Evol. Comput., vol. 1, no. 1, pp. 67–82, 1997, doi: 10.1109/4235.585893.

[80] L. Liu, M. Khishe, M. Mohammadi, and A. H. Mohammed, Optimization of constraint engineering problems using robust universal learning chimp optimization, Adv. Eng. Informatics, vol. 53, p. 101636, 2022.

[81] S.-P. Gong, M. Khishe, and M. Mohammadi, Niching Chimp Optimization for Constraint Multimodal Engineering Optimization Problems, Expert Syst. Appl., p. 116887, 2022.

[82] R. Poláková, L-SHADE with competing strategies applied to constrained optimization, in 2017 IEEE congress on evolutionary computation (CEC), IEEE, 2017, pp. 1683–1689.

[83] A. A. Hadi, A. W. Mohamed, and K. M. Jambi, Single-objective real- parameter optimization: Enhanced LSHADE-SPACMA algorithm, in Heuristics for optimization and learning, Springer, 2021, pp. 103–121.

[84] K. Krishnamoorthy, Wilcoxon Signed- Rank Test, in Handbook of Statistical Distributions with Applications, 2020, pp. 339–342. doi: 10.1201/9781420011371-34.

[85] H. Abdi, Holm's sequential Bonferroni procedure, Encycl. Res. Des., vol. 1, no. 8, pp. 1–8, 2010.

[86] G. A. Mack and J. H. Skillings, A Friedman-type rank test for main effects in a two-factor ANOVA, J. Am. Stat. Assoc., vol. 75, no. 372, pp. 947–951, 1980.

[87] P. N. Price, K. V., Awad, N. H., Ali, M. Z., & Suganthan, Problem definitions and evaluation criteria for the 100-digit challenge special session and competition on single objective numerical optimization. Technical Report., 2018. [Online]. Available: https://personal.ntu.edu.sg/404.html

[88] A. Kumar, G. Wu, M. Z. Ali, R. Mallipeddi, P. N. Suganthan, and S. Das, A test-suite of non-convex constrained optimization problems from the real-world and some baseline results, Swarm Evol. Comput., 2020, doi: 10.1016/j.swevo.2020.100693.

[89] L. Yin, S. Lin, Z. Sun, S. Wang, R. Li, and Y. He, PriMonitor: An adaptive tuning privacy-preserving approach for multimodal emotion detection, World Wide Web, vol. 27, no. 2, pp. 1–28, 2024.

[90] L. Yin, S. Lin, Z. Sun, R. Li, Y. He, and Z. Hao, A game-theoretic approach for federated learning: a trade-off among privacy, accuracy and energy, Digit. Commun. Networks, vol. 10, no. 2, pp. 389–403, 2024.

[91] H. Liu, T. Xue, and T. Schultz, Merged Pitch Histograms and Pitch- duration Histograms., in SIGMAP, 2022, pp. 32–39.

[92] J. Brest, M. S. Maucec, and B. Boskovic, The 100-Digit Challenge: Algorithm jDE100, in 2019 IEEE Congress on Evolutionary Computation, CEC 2019 - Proceedings, 2019. doi: 10.1109/CEC.2019.8789904.

[93] S. X. Zhang, W. Shing Chan, K. S. Tang, and S. Yong Zheng, Restart based Collective Information Powered Differential Evolution for Solving the 100-Digit Challenge on Single Objective Numerical Optimization, in 2019 IEEE Congress on Evolutionary Computation, CEC 2019 - Proceedings, 2019. doi: 10.1109/CEC.2019.8790279.

[94] J. F. Yeh, T. Y. Chen, and T. C. Chiang, Modified L-SHADE for Single Objective Real-Parameter Optimization, in 2019 IEEE Congress on Evolutionary Computation, CEC 2019 - Proceedings, 2019. doi: 10.1109/CEC.2019.8789991.

[95] D. Yazdani, R. Cheng, D. Yazdani, J. Branke, Y. Jin, and X. Yao, A survey of evolutionary continuous dynamic optimization over two decades—Part A, IEEE Trans. Evol. Comput., vol. 25, no. 4, pp. 609–629, 2021.

[96] J. Branke and H. Schmeck, Designing evolutionary algorithms for dynamic optimization problems, Adv. Evol. Comput. theory Appl., pp. 239–262, 2003.

[97] T. Blackwell and J. Branke, Multiswarms, exclusion, and anti- convergence in dynamic environments, IEEE Trans. Evol. Comput., vol. 10, no. 4, pp. 459–472, 2006.

Meng Yu, received his Bachelor's degree from Liaoning University and Master's degree from Dalian University of Technology. He is currently teaching in Anshan Normal University, mainly researching on the application of machine learning algorithms in network security protection, and is committed to building a safer and smarter network environment.
https://orcid.org/0009-0003-1219-5423

Mohammad Khishe received a B.Sc. degree in Maritime Electronics and Communication Engineering from Imam Khomeini Maritime Sciences University, Nowshahr, Iran in 2007 and also, M.Sc. and Ph. D. degrees in Electronic Engineering from Islamic Azad University, Qazvin branch, and Iran University of Science and Technology, Tehran in 2012 and 2017, respectively. Currently, he is associate professor at Imam Khomeini Maritime Sciences University, Nowshahr, Iran. His research interests are Optimization, Artificial Neural Networks, Meta-heuristic Algorithms, Sonar and Radar Signal Processing. He is Listed among Top 2% scientists in the world, [Courtesy: Stanford University]
https://orcid.org/0000-0002-1024-8822

Leren Qian is a researcher specializing in Operations Research and Artificial Intelligence. He holds an M.Sc. in Computer Science with a focus on AI, and a Ph.D. in Operations Research with a concentration in engineering optimization. His current research interests include applied machine learning, engineering optimization, and the design of meta-heuristic algorithms.

Diego Martín received the B.Sc. degree in computer engineering, the M.Sc. degree in computer science from the Department of Informatics, Carlos III University of Madrid, Madrid, Spain. He received the Ph.D. degree from the Department of Informatics, Carlos III University of Madrid, in 2012. He is currently a Lecturer with the Department of Telematics, Technical University of Madrid (UPM), Madrid. His research interests during his collaborations in the STRAST and GISAI research groups, at UPM, are Internet of Things, cyberphysical systems, physically unclonable functions, blockchain, knowledge management, information retrieval, and research methods.
https://orcid.org/0000-0001-8810-0695

Laith Abualigah is the Director of the Department of International Relations and Affairs at Al Al-Bayt University, Jordan. He is an Associate Professor at the Computer Science Department, Al Al-Bayt University, Jordan. He is also a distinguished researcher at many prestigious universities. He received a Ph.D. degree from the School of Computer Science at Universiti Sains Malaysia (USM), Malaysia, in 2018. According to the report published by Clarivate, He is one of the Highly Cited Researchers in 2021-2023 and the 1\% influential Researcher, which depicts the 6,938 top scientists in the world. In addition, the first researcher in the domain of Computer Science in Jordan for 2021-2023. According to the report published by Stanford University, He is one of the 2\% influential scholars, which depicts the 100,000 top scientists in the world. He has published more than 500 journal papers and books, which collectively have been cited more than 20900 times (H-index = 64). His main research interests focus on Artificial Intelligence, Meta-heuristic Modeling, and Optimization Algorithms, Evolutionary Computations, Information Retrieval, Text clustering, Feature Selection, Combinatorial Problems, Optimization, Advanced Machine Learning, Big data, and Natural Language Processing. He currently serves as an associate editor of many prestigious Journals in Elsevier, Springer, ACM, IEEE, and others.
https://orcid.org/0000-0002-2203-4549

Taher M. Ghazal, a distinguished IEEE Senior Member, is a seasoned academician with a comprehensive educational background. He earned his Bachelor of Science degree in Software Engineering from Al Ain University in 2011, followed by a Master of Science degree in Information Technology Management from The British University in Dubai, associated with The University of Manchester and The University of Edinburgh in 2013. Dr. Ghazal culminated his academic journey with a Doctorate in Information Science and Technology from Universiti Kebangsaan Malaysia in 2023. Possessing over a decade of multifaceted expertise, Dr. Ghazal has fulfilled various roles including lecturer, instructor, tutor, researcher, teacher, IT support/specialist engineer, and business/systems analyst. He has contributed significantly across diverse departments such as Engineering, Computer Science, ICT, and as Head of STEM and Innovation. His professional engagements have extended to governmental and private educational institutions under the purview of KHDA, Ministry of Education, and Ministry of Higher Education and Scientific Research, UAE. Dr. Ghazal's scholarly pursuits encompass a wide array of interests including IoT, Artificial Intelligence, Cybersecurity, Information Systems, Software Engineering, Web Development, Building Information Modeling, Quality of Education, Management, Big Data, Quality of Software, and Project Management. He is actively engaged in community service through his involvement in impactful projects and research endeavors.
https://orcid.org/ 0000-0003-0672-7924